



# Comparative Analysis of Magnetohydrodynamic Inclined Poiseuille Flow of Couple Stress Fluids

Muhammad Farooq <sup>a</sup>, Atiq Ur Rahman <sup>a</sup>, Asfandyar Khan <sup>a</sup>, Ilker Ozsahin <sup>b</sup>, Berna Uzun <sup>b, c</sup>,  
Hijaz Ahmad <sup>\*, b, d</sup>

<sup>a</sup> Department of Mathematics, Abdul Wali Khan University, Mardan, KP, 23200, Pakistan

<sup>b</sup> Operational Research Center in Healthcare, Near East University, 99138, Nicosia/TRNC Mersin 10, Turkey

<sup>c</sup> Department of Mathematics, Faculty of Arts and Sciences, Near East University, 99138, Nicosia/TRNC Mersin 10, Turkey

<sup>d</sup> Department of Mathematics, College of Science, Korea University, 145 Anam-ro, Seongbuk-gu, Seoul 02841, South Korea

## Abstract

**In this paper, the inclined Poiseuille flow of a couple stress fluid between two parallel plates under the influence of a magnetic field is investigated using two analytical techniques: the Homotopy Analysis Method (HAM) and the Optimal Auxiliary Function Method (OAFM). The effects of various non-dimensional parameters on the velocity profile, temperature distribution, shear stresses, and flow rate are analysed in detail. The solutions obtained from HAM and OAFM are compared through graphical and tabular representations, including residual error analysis. The results demonstrate that OAFM provides a more efficient and accurate solution than HAM. Ultimately, we conclude that both methods are effective in solving highly nonlinear differential equations and complex physical models.**

**Keywords:** Couple Stress Fluid; Poiseuille Flow; Optimal Auxiliary Function Method; Homotopy Analysis Method; Magnetohydrodynamic

## 1. Introduction

Magnetohydrodynamics (MHD) has numerous applications in both biological and engineering sciences, playing a crucial role in various fluid flow problems. Its applications extend beyond fluid mechanics to a wide range of engineering disciplines. For instance, Kumar *et al.*[1] analyzed fluid flow across a stretching cylinder under the influence magnetic dipole. Gowda *et al.* [2] investigated the MHD effect using magnetized flow, heat diffusion theory, and Stefan blowing conditions. In another study, Gowda *et al.* [3] examined the contribution of MHD flow across a stretching sheet to the fluid flow influenced by the magnetic dipole. Magneto bioconvection flow across an inclined plate with entropy generation was discussed by Yusuf *et al.*[4]. The effect of MHD on thermophoretic particles in the fluid flow over a stretching sheet was discussed by Kumar *et al.*[5]. The flow of a squeezed nanofluid between two plates was investigated by Domairry and Hatami [6]. Pourmehran *et al.*[7] have researched the squeezing flow that occurs when two parallel plates are squeezed together. Khan *et al.*[8] have expanded on this analysis by taking the viscous dissipation features into consideration. The effect of a magnetic field on an electrically conducting fluid, such as water, is known as magnetohydrodynamics (MHD), and it has just been introduced [9]. MHD cooling reactors, castings, and sensors all have extensive uses in industry and engineering. The influence of couple stress on pulsatile hydromagnetic Poiseuille flow was discussed by El-Dabe and El-Mohandis

\* Corresponding author.: hijaz.ahmad@neu.edu.tr

[10]. Farooq *et al.*[11] investigated the laminar flow of couple stress fluids using Vogel's model. In an inclined magnetic field, Manyonge *et al.*[12] describe steady Poiseuille flow between two infinitely parallel porous plates.

A linearization or discretization process is generally used in numerical methods, which can result in divergent solutions in some cases. The efficiency of OAFM can be demonstrated by comparing its numerical results with those produced by the Runge-Kutta method of order 4. OAFM is a new optimization methodology developed by Herisanu [13, 14] that does not require linearization, discretization, or problems with small parameters as is the case with perturbation methods. The large convergence region of the OAFM is controlled by an optimal constant. It produces an accurate response after one iteration without the need for complicated mathematical techniques, and even low-spec computers are capable of running it. Additionally, OAFM is easy to use and quickly converges when compared to other semi-analytical methods such as HAM and OHAM. According to Reference. [15], Optimal Auxiliary Function Method (OAFM) is used to solve the nonlinear differential equations that describe the Blasius problem. In Reference [16], the Optimal Auxiliary Function Method (OAFM) is used to roughly solve the thin film flow problem on a moving belt. In reference [17], an analytical approach to the Optimal Auxiliary Function Method may be applied to the boundary nonlinear problem resulting from a stretching surface with partial slip. The OAFM is used in Reference [18] to investigate the nonlinear oscillations of a pendulum wrapped around two cylinders. Using Lax's seventh-order Kdv and Sawadara Kotera equations as an approximate solution, the OAFM is extended to partial differential equations (PDEs) in Ref. [19].

The Homotopy Analysis Method (HAM), which is proposed by Liao [20] is used for the solution of nonlinear problems. Srinivasacharya and Kaladhar [21, 22] provide examples of the methodology and current advances of the HAM. Ramzan *et al.*[23] solved the three-dimensional couple stress fluid flow with Newtonian heating analytically by using the Homotopy Analysis Method (HAM). Khan *et al.*[24] research considered the numerical solution of a spinning disk's fluid flow through a time-dependent magneto hydrodynamic coupling stress. The analytical solution of a three-dimensional magnetohydrodynamic couple stress nanofluid flow across a nonlinear stretched surface with convective heat and mass boundary conditions was well thought out by Hayat *et al.*[25]. Ramzan *et al.*[26] used the HAM to find a set of solutions for three-dimensional couple stress nanofluid flow with joule heating. It was recently reported by Hayat *et al.*[27] that a three-dimensional magnetohydrodynamic coupled stress nanofluid flow accompanied by heat generation and absorption under convective conditions could be solved as a series solution.

Couple stress fluid model is one of the many viscoelastic fluid models that have been proposed and depicted the behavior of non-Newtonian fluids. Couple stresses and body couples are included in the couple stress fluid model, which are the generalization of the classical fluid model (i.e., the viscous fluid) [28]. Blood from both humans and animals, colloidal fluids, liquid crystals and fluids with long-chain molecules are a few examples of couple stress fluids. In these kinds of fluids, the constitutive equations essentially link the angular component of velocity to the gradient of angular velocity and the skew-symmetric component of the stress tensor to the couple stress. The Navier-Stokes equations cannot be used to simulate coupled stress fluids because their stress tensor is not symmetric. Fluids with solid particles suspended in a viscous medium, such as blood, lubricants containing a small amount of polymer preservative, and synthetic fluids with solid particles can all be considered couple stress fluids [29]. Many researchers have recently used couple stress fluids in their investigations due to the importance of these fluids. In this investigation, Hadjesfandiari and Dargush [30] looked at various iterations of couple stress fluid. A permeable medium with peristaltic hemodynamics and a slip effect at the boundary were studied by Tripathi [31] in his investigation of couple stress fluid. Solutions for CSF flows under slip boundary conditions were derived by Devakar *et al.*[32]. They investigated many different kinds of examples in their study, including (Poiseuille, Couette and generalized Couette flow). In this study, the couple stress parameter was found to be responsible for the retardation of fluid velocity. Ramanaiah *et al.*[33] investigated the effects of CSF lubrication on the squeezing films. Accordingly, he concluded that squeeze times were increased when CSF was used as a lubricant. Chippa and Sarangi [34]. It has been shown that incompressible CSF flows across porous materials by Alsaedi *et al.*[35]. As a function of the CSF parameter, they also examined the expressions of several parameters. Basha *et al.*[36] present numerical solutions for the transient two-dimensional natural convection of CSF flow past a vertical plate. The solutions for CSF moving hydromagnetic peristaltically through a porous channel were investigated by Reddy *et al.*[37]. According to Awais *et al.*[38], CSF flow on a convective sliding surface was investigated.

In this study, we consider the steady flow of couple stress fluid between two infinitely parallel inclined plates under the impact of MHD. We use the two well-known techniques of HAM and OAFM to investigate this problem. Section 2 provide nomenclature Basic equations are provided in Section 3. Problem formulation is mentioned in Section 4. Section 5 discussed the methodology of the proposed approach. Sections 6 and 7 contain solutions to the suggested model. We calculate the volume flux, average velocity, and shear stress on the plates in Section 8. Results and discussions of the suggested problem are given in Section 9. The conclusion is provided in Section 10.

## 2. Nomenclature

$\Phi$  = velocity vector  
 $\varphi$  = temperature  
 $U$  = characteristic velocity  
 $I$  = unit tensor  
 $f$  = body force  
 $S$  = Hight of plates  
 $U$  = dimensional velocity in the x-direction  
 $U^*$  = non- dimensional velocity in the x-direction  
 $\delta$  = Dimensional y-coordinate  
 $\delta^*$  = non-dimensional y-coordinates  
 $\epsilon$  = Small parameter  
 $\eta$  = Couple stress parameter  
 $\varphi$  = Dimensional temperature  
 $\varphi^*$  = Dimensionless temperature  
 $\varphi_0$  = Lower plate temperature  
 $\varphi_1$  = Upper plate temperature  
 $\kappa$  = Thermal conductivity  
 $\mu_0$  = Dimensional coefficient of viscosity  
 $\rho$  = Constant density of the fluid

## 3. Basic Equation

An incompressible couple stress fluid flow according to the following basic equations are

$$\text{div}.\Phi = 0, \quad (1)$$

$$\rho \frac{D\Phi}{Dt} = \text{div}.T_1 + \eta \nabla^4 \Phi + \rho f + j \times \beta, \quad (2)$$

$$\rho c_p \frac{D\varphi}{Dt} = k \nabla^2 \varphi + T_1.E. \quad (3)$$

Where  $\Phi$  is the velocity vector,  $E$  is the gradient of  $\Phi$ ,  $\eta$  is the couple stress parameter,  $c_p$  is the specific heat,  $\rho$  is the constant density,  $f$  is the body force per-unit mass,  $T_1$  is the Cauchy stress tensor,  $\varphi$  is the temperature,  $k$  is the thermal conductivity and the operator  $\frac{D}{Dt}$  denotes the material time derivative which is define as:

$$\frac{D}{Dt} (*) = \left( \frac{\partial}{\partial t} + V.\nabla \right) (*),$$

The Cauchy stress tensor  $A_1$  can be define as:

$$T_1 = -pI + \tau, \quad \tau = \mu A_1, \quad (4)$$

Where  $p$  is the dynamic pressure,  $\mu$  is the coefficient of viscosity,  $I$  is the unit tensor and  $A_1$  is the first Rivlin-Erickson tensor which is define as:

$$A_1 = q + q^T, \quad q^T \text{ is the transpose of } q.$$

## 4. Formulation and Solution of Inclined Poiseuille Flow

The steady MHD Poiseuille flow over two parallel inclined plates are studied in this article; the flow is influenced by both gravity and a constant pressure gradient. The distance between the two plates is  $2S$ . Where  $\delta =$

-S and  $\delta = S$ , respectively, represent the lower and upper plates of the channel. In Fig. 1, we show the model chosen coordinate system and geometrical skew.

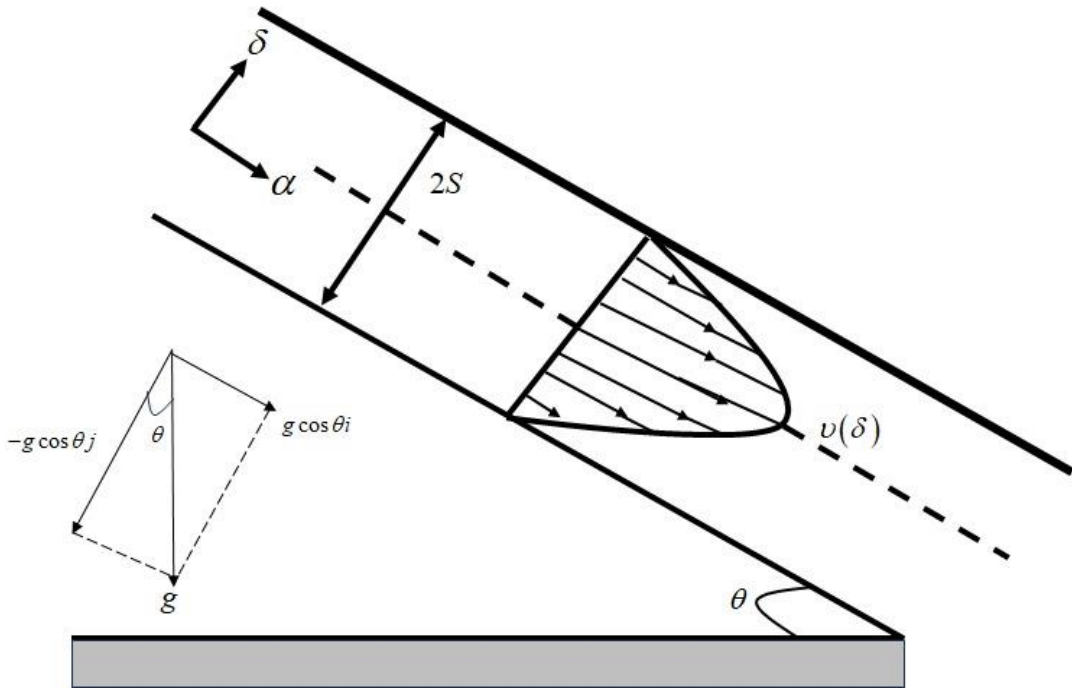


Figure 1: Geometry of the problem

$$\Phi = \Phi(v, 0, 0), \quad v = v(\delta) \text{ and } \varphi = \varphi(\delta). \tag{5}$$

Using these assumptions, we observe that the continuity Eq. (1) is identically satisfied and the momentum Eq. (2) reduced to

$$0 = -\frac{\partial p}{\partial \alpha} + \frac{\partial}{\partial \delta}(\tau_{\alpha\delta}) - \eta \frac{d^4 v}{d\delta^4} + \rho g \sin \theta - \sigma \beta_0^2 v, \tag{6}$$

$$0 = -\frac{\partial p}{\partial \delta} - \sigma g \cos \theta, \tag{7}$$

$$0 = -\frac{\partial p}{\partial \gamma}. \tag{8}$$

Eq. (11) implies that  $p \neq p(\gamma)$  using Eq. (5) in Eq. (4) the non- zero components of the extra stress tensor are

$$\tau_{\alpha\delta} = \mu \frac{dv}{d\delta} = \tau_{\delta\alpha}. \tag{9}$$

Substituting Eq. (9) into Eq. (6) we obtain

$$\eta \frac{d^4 v}{d\delta^4} - \mu \frac{d^2 v}{d\delta^2} - \frac{d\mu}{d\delta} \frac{dv}{d\delta} + \frac{\partial p}{\partial \alpha} - \rho g \sin \theta + \sigma \beta_0^2 v = 0. \tag{10}$$

Eq. (4), (5) and Eq. (9) change the form of energy equation Eq. (3) to the form

$$\frac{d^2 \varphi}{d\delta^2} + \frac{\mu}{k} \left( \frac{dv}{d\delta} \right)^2 + \frac{\eta}{k} \left( \frac{d^2 v}{d\delta^2} \right) = 0. \tag{11}$$

The associate boundary conditions are

$$\nu(-s) = \nu(s) = 0, \quad (12)$$

$$\nu''(-s) = \nu''(s) = 0, \quad (13)$$

$$\varphi(-s) = \varphi_0, \quad \varphi(s) = \varphi_1. \quad (14)$$

Eq. (12) is the usual no-slip boundary condition Eq. (11) implies that couple stress is zero at the plates. We introduce the following non-dimensional parameters:

$$\nu^* = \frac{\nu}{U}, \quad \delta^* = \frac{\delta}{S}, \quad \alpha^* = \frac{\alpha}{S}, \quad \varphi^* = \frac{\varphi - \varphi_0}{\varphi_1 - \varphi_0}, \quad \mu^* = \frac{\mu}{\mu_0}, \quad p^* = \frac{p}{\mu_0 U / S},$$

$$B_r = \frac{\mu_0 U^2}{k(\varphi_1 - \varphi_0)}, \quad B^2 = \frac{\mu_0 S^2}{\eta}, \quad G = -\frac{B^2 S^5}{\mu_0 U} \frac{\partial p}{\partial \alpha} + \frac{\rho g S^4}{\eta U} \sin \theta, \quad \Gamma = \frac{\sigma \beta_0^2 B^2 S^2}{\mu_0}.$$

Where  $\mu_0$  is the reference viscosity,  $U$  is the characteristic velocity and  $B_r$  is the Brinkman number. Using these dimensionless parameters in Eq. (10) and (11) take the form

$$\frac{d^4 \nu}{d\delta^4} - B^2 \mu \frac{d^2 \nu}{d\delta^2} - B^2 \frac{d\mu}{d\delta} \frac{d\nu}{d\delta} + \Gamma \nu - G = 0 \quad (15)$$

$$\frac{d^2 \varphi}{d\delta^2} + B_r \mu \left( \frac{d\nu}{d\delta} \right)^2 + \frac{B_r}{B^2} \left( \frac{d^2 \nu}{d\delta^2} \right)^2 = 0. \quad (16)$$

And the corresponding boundary condition (12)-(14) become.

$$\nu(-1) = 0, \quad \nu(1) = 0, \quad (17)$$

$$\nu''(-1) = 0, \quad \nu''(1) = 0, \quad (18)$$

$$\varphi(-1) = 0, \quad \varphi(1) = 1. \quad (19)$$

Assume that the Reynolds' model [21-25, 39-42] provides the temperature-dependent fluid viscosity. The model's dimensionless form is [43, 44].

$$\mu = \exp(-M\varphi). \quad (20)$$

Using the Taylor series expansion, Eq. (20) reduce to

$$\mu \cong 1 - M\varphi, \quad \frac{d\mu}{d\delta} \cong -M \frac{d\varphi}{d\delta}. \quad (21)$$

Substituting Eq. (21) in the governing Eq. (15) and (16) the following couple system is obtained

$$\frac{d^4 \nu}{d\delta^4} - B^2 (1 - M\varphi) \frac{d^2 \nu}{d\delta^2} + B^2 M \frac{d\varphi}{d\delta} \frac{d\nu}{d\delta} + \Gamma \nu - G = 0, \quad (22)$$

$$\frac{d^2 \varphi}{d\delta^2} + B_r (1 - M\varphi) \left( \frac{d\nu}{d\delta} \right)^2 + \frac{B_r}{B^2} \left( \frac{d^2 \nu}{d\delta^2} \right)^2 = 0. \quad (23)$$

## 5. Basics of the Proposed Method

### 5.1. Methodology of OAFM

We consider the most general form of a non-linear differential equation as

$$L[\Phi(v)] + N[\Phi(v)] = 0. \tag{24}$$

Where L represents the linear operator, N represents the non-linear operator, and  $\Phi(v)$  is a given function. The initial or boundary condition is known as

$$B\left(\Phi(v), \frac{d\Phi(v)}{dv}\right) = 0. \tag{25}$$

For Eq. (24) and (25) the approximate solution can be written as

$$\Phi^*(v, C_i) = \Phi_0(v) + \Phi_1(v, C_i), \quad i = 1, 2, 3, \dots, n. \tag{26}$$

Substituting Eq. (26) into Eq. (24) we get

$$L[\Phi_0(v) + \Phi_1(v, C_i)] + N[\Phi_0(v) + \Phi_1(v, C_i)] = 0. \tag{27}$$

The linear term can be used to get the initial approximation  $\Phi_0(v)$  is

$$L[\Phi_0(v)] = 0, \quad B\left(\Phi_0(v), \frac{d\Phi_0(v)}{dv}\right) = 0. \tag{28}$$

Now to find the value of first approximation from the remaining equation

$$L[\Phi_1(v, C_i)] + N[\Phi_0(v) + \Phi_1(v, C_i)] = 0, \quad B\left(\Phi_1(v), \frac{d\Phi_1(v)}{dv}\right) = 0. \tag{29}$$

The non-linear term from Eq. (29) is expanded in the form

$$N[\Phi_0(v) + \Phi_1(v, C_i)] = N[\Phi_0(v)] + \sum_{k \geq 1} \frac{\Phi_1^k(v, C_i)}{k!} N^k[\Phi_0(v)], \quad N^k = \frac{d^k N}{dv^k}. \tag{30}$$

Instead of the last term arising in Eq. (29), we propose another expression, allowing Eq. (29) to be written in a new form, in order to avoid the challenges that arise when solving the nonlinear differential equation (29) and to speed up the convergence of the first approximation and implicitly of the approximate solution  $\Phi^*(v, C_i)$

$$L[\Phi_1(v, C_i)] + A_1(\Phi_0(v, C_j))P[N(\Phi_0(v))] + A_2(\Phi_0(v), C_k) = 0, \tag{31}$$

$$B\left(\Phi_1(v), \frac{d\Phi_1(v)}{dv}\right) = 0, \tag{32}$$

Where  $A_1$  and  $A_2$  are arbitrary auxiliary functions that depend on the initial approximation of  $\Phi_0(v)$  and a number of unknown parameters,  $C_i, C_j$  and  $C_k$ .  $j = 1, 2, \dots, p, k=p+1, p+2, \dots, n$ , and  $i = j+k$ . where  $i = 1, 2, \dots, n$ ,  $P[N(\Phi_0(v))]$  denotes a component of the operator  $N[\Phi_0(v)]$ . The auxiliary functions  $A_1$  and  $A_2$  called optimal auxiliary functions are not unique and can take on the same form as of  $\Phi_0(v)$  or  $N[\Phi_0(v)]$  or a combination of both of  $\Phi_0(v)$  and  $N[\Phi_0(v)]$ . By using several techniques, the unknown parameters  $C_j$  and  $C_k$  can be recognized in the best possible way. They include minimizing the square residual error.

$$j(C_i, C_k) = \int_{(D)} R^2(v, C_i, C_k) dv. \tag{33}$$

Where  $R(v, C_i, C_k) = L[\Phi^*(v, C_i)] + N[\Phi^*(v, C_i)]$ ,  $j = 1, 2, \dots, p, k=p+1, p+2, \dots, n$ , and  $i = j+k$ . The condition of the minimization of the result are

$$\frac{\partial j}{\partial C_1} = \frac{\partial j}{\partial C_2} = \dots = \frac{\partial j}{\partial C_n} = 0. \tag{34}$$

To find the values of the unknown parameters we also use different methods either by Ritz method, Collocation method, Galerkin method or Kantorovich method.

### 6. Solution of the Problem Using OAFM

As of the first component, the OAFM solutions for velocity and temperature are shown below.

Zeroth component problems are listed below

$$\frac{d^4 v_0}{d\delta^4} - G = 0, \quad (35)$$

$$v_0(-1) = 0, v_0(1) = 0, v_0''(-1) = 0, v_0''(1) = 0, \quad (36)$$

$$\frac{d^2 \varphi_0}{d\delta^2} = 0, \quad (37)$$

$$\varphi_0(-1) = 0, \varphi_0(1) = 1. \quad (38)$$

The solution of these problem is

$$v_0 = \frac{1}{24}(5G - 6G\delta^2 + G\delta^4), \quad (39)$$

$$\varphi_0 = \frac{1 + \delta}{2}. \quad (40)$$

The non-linear part is given by

$$N(v) = -B^2(1 - M\varphi)\partial_{\delta,\delta}v + B^2M\partial_{\delta}\varphi\partial_{\delta}v + \Gamma v. \quad (41)$$

Substituting  $v_0$  and  $\varphi_0$  in Eq. (44), we obtain

$$N(v_0) = -B^2(1 - M\varphi_0)\partial_{\delta,\delta}v_0 + B^2M\partial_{\delta}\varphi_0\partial_{\delta}v_0 + \Gamma v_0. \quad (42)$$

Also

$$A_1 = c_1 \left( \frac{1 + \delta}{2} \right)^2 + c_2 \left( \frac{1 + \delta}{2} \right)^4, \quad A_2 = 0. \quad (43)$$

The first approximation  $v_1$  can be obtain as

$$\frac{d^4 v_1}{d\delta^4} + A_1 N(v_0) + A_2 N(v_0, C_j) = 0, \quad (44)$$

$$v_1(-1) = 0, v_1(1) = 0, v_1''(-1) = 0, v_1''(1) = 0, \quad (45)$$

Using Eq. (39), Eq. (40) and Eq. (42) into Eq. (44), we get

$v_1 =$

$$\begin{aligned} & \frac{1}{31933440} (-767448B^2Gc_1 + 608652B^2GMc_1 - 309738G\Gamma c_1 - 98208B^2G\delta c_1 + 126544B^2GM\delta c_1 - \\ & 38588G\Gamma\delta c_1 + 931392B^2G\delta^2 c_1 - 709632B^2GM\delta^2 c_1 + 377190G\Gamma\delta^2 c_1 + 155232B^2G\delta^3 c_1 - \\ & 189024B^2GM\delta^3 c_1 + 61776G\Gamma\delta^3 c_1 - 166320B^2G\delta^4 c_1 + 83160B^2GM\delta^4 c_1 - 69300G\Gamma\delta^4 c_1 - \\ & 66528B^2G\delta^5 c_1 + 66528B^2GM\delta^5 c_1 - 27720G\Gamma\delta^5 c_1 + 22176B^2GM\delta^6 c_1 + 924G\Gamma\delta^6 c_1 + \\ & 9504B^2G\delta^7 c_1 - 3168B^2GM\delta^7 c_1 + 4752G\Gamma\delta^7 c_1 + 2376B^2G\delta^8 c_1 - 4356B^2GM\delta^8 c_1 + \\ & 990G\Gamma\delta^8 c_1 - 880B^2GM\delta^9 c_1 - 220G\Gamma\delta^9 c_1 - 66G\Gamma\delta^{10} c_1 - 313038B^2Gc_2 + 309903B^2GMc_2 - \\ & 124601G\Gamma c_2 - 63096B^2G\delta c_2 + 76622B^2GM\delta c_2 - 24642G\Gamma\delta c_2 + 365310B^2G\delta^2 c_2 - \\ & 347391B^2GM\delta^2 c_2 + 145992G\Gamma\delta^2 c_2 + 95040B^2G\delta^3 c_2 - 106172B^2GM\delta^3 c_2 + 37598G\Gamma\delta^3 c_2 - \\ & 41580B^2G\delta^4 c_2 + 20790B^2GM\delta^4 c_2 - 17325G\Gamma\delta^4 c_2 - 33264B^2G\delta^5 c_2 + 24948B^2GM\delta^5 c_2 - \end{aligned}$$

$$13860G\Gamma \delta^5 c_2 - 13860B^2G\delta^6 c_2 + 18018B^2GM\delta^6 c_2 - 5544G\Gamma \delta^6 c_2 + 6336B^2GM\delta^7 c_2 + 396G\Gamma \delta^7 c_2 + 2970B^2G\delta^8 c_2 - 693B^2GM\delta^8 c_2 + 1485G\Gamma \delta^8 c_2 + 1320B^2G\delta^9 c_2 - 1650B^2GM\delta^9 c_2 + 550G\Gamma \delta^9 c_2 + 198B^2G\delta^{10} c_2 - 627B^2GM\delta^{10} c_2 - 84B^2GM\delta^{11} c_2 - 42G\Gamma \delta^{11} c_2 - 7G\Gamma \delta^{12} c_2). \quad (46)$$

Adding Eq. (39) and Eq. (46) Our approximation's outcome up to the first component is.

$$\begin{aligned} v_{OAFM} = & \frac{1}{24} (5G - 6G\delta^2 + G\delta^4) + \frac{1}{31933440} (-767448B^2Gc_1 + 608652B^2GMc_1 - 309738G\Gamma c_1 - \\ & 98208B^2G\delta c_1 + 126544B^2GM\delta c_1 - 38588G\Gamma \delta c_1 + 931392B^2G\delta^2 c_1 - 709632B^2GM\delta^2 c_1 + \\ & 377190G\Gamma \delta^2 c_1 + 155232B^2G\delta^3 c_1 - 189024B^2GM\delta^3 c_1 + 61776G\Gamma \delta^3 c_1 - \\ & 166320B^2G\delta^4 c_1 + 83160B^2GM\delta^4 c_1 - 69300G\Gamma \delta^4 c_1 - 66528B^2G\delta^5 c_1 + 66528B^2GM\delta^5 c_1 - \\ & 27720G\Gamma \delta^5 c_1 + 22176B^2GM\delta^6 c_1 + 924G\Gamma \delta^6 c_1 + 9504B^2G\delta^7 c_1 - \\ & 3168B^2GM\delta^7 c_1 + 4752G\Gamma \delta^7 c_1 + 2376B^2G\delta^8 c_1 - 4356B^2GM\delta^8 c_1 + 990G\Gamma \delta^8 c_1 - \\ & 880B^2GM\delta^9 c_1 - 220G\Gamma \delta^9 c_1 - 66G\Gamma \delta^{10} c_1 - 313038B^2Gc_2 + 309903B^2GMc_2 - \\ & 124601G\Gamma c_2 - 63096B^2G\delta c_2 + 76622B^2GM\delta c_2 - 24642G\Gamma \delta c_2 + 365310B^2G\delta^2 c_2 - \\ & 347391B^2GM\delta^2 c_2 + 145992G\Gamma \delta^2 c_2 + 95040B^2G\delta^3 c_2 - 106172B^2GM\delta^3 c_2 + 37598G\Gamma \delta^3 c_2 - \\ & 41580B^2G\delta^4 c_2 + 20790B^2GM\delta^4 c_2 - 17325G\Gamma \delta^4 c_2 - 33264B^2G\delta^5 c_2 + 24948B^2GM\delta^5 c_2 - \\ & 13860G\Gamma \delta^5 c_2 - 13860B^2G\delta^6 c_2 + 18018B^2GM\delta^6 c_2 - 5544G\Gamma \delta^6 c_2 + 6336B^2GM\delta^7 c_2 + \\ & 396G\Gamma \delta^7 c_2 + 2970B^2G\delta^8 c_2 - 693B^2GM\delta^8 c_2 + 1485G\Gamma \delta^8 c_2 + \\ & 1320B^2G\delta^9 c_2 - 1650B^2GM\delta^9 c_2 + 550G\Gamma \delta^9 c_2 + 198B^2G\delta^{10} c_2 - \\ & 627B^2GM\delta^{10} c_2 - 84B^2GM\delta^{11} c_2 - 42G\Gamma \delta^{11} c_2 - 7G\Gamma \delta^{12} c_2). \end{aligned} \quad (47)$$

The non-linear component of the energy equation is denoted as

$$N(\varphi) = B_r (1 - M\varphi)(\partial_\delta v)^2 + \frac{B_r}{B^2} (\partial_{\delta,\delta} v)^2. \quad (48)$$

The same method can also be used to determine the value of  $v$  and  $\varphi$  when  $v_0$  and  $\varphi_0$  are substituted in Eq. (48), we obtain

$$N(\varphi_0) = B_r (1 - M\varphi_0)(\partial_\delta v_0)^2 + \frac{B_r}{B^2} (\partial_{\delta,\delta} v_0)^2, \quad (49)$$

$$A_3 = c_3 \left( \frac{1 + \delta}{2} \right)^6 + c_4 \left( \frac{1 + \delta}{2} \right)^8, \quad A_4 = 0. \quad (50)$$

The first approximation  $\varphi_1$  can be obtain as

$$\frac{d^2 \varphi_1}{d\delta^2} + A_1 N(\varphi_0) + A_2 N(\varphi_0, C_j) = 0, \quad (51)$$

$$\varphi_1(-1) = 0, \quad \varphi_1(1) = 0. \quad (52)$$

Using Eq. (40), Eq. (49) and Eq. (50) into Eq. (51), we get

$$\begin{aligned} \varphi_1 = & \frac{1}{225833287680B^2} (898646112G^2 B_r c_3 + 510847008B^2G^2 B_r c_3 - 432665232B^2G^2 M B_r c_3 + \\ & 793054080G^2 \delta B_r c_3 + 508540992B^2G^2 \delta B_r c_3 - 431818768B^2G^2 M \delta B_r c_3 - 441080640G^2 \delta^2 B_r c_3 - \end{aligned}$$

$$\begin{aligned}
& 882161280G^2\delta^3B_{r,c_3} - 955674720G^2\delta^4B_{r,c_3} - 73513440B^2G^2\delta^4B_{r,c_3} + 36756720B^2G^2M\delta^4B_{r,c_3} - \\
& 352864512G^2\delta^5B_{r,c_3} - 264648384B^2G^2\delta^5B_{r,c_3} + 154378224B^2G^2M\delta^5B_{r,c_3} + \\
& 411675264G^2\delta^6B_{r,c_3} - 421477056B^2G^2\delta^6B_{r,c_3} + 298954656B^2G^2M\delta^6B_{r,c_3} + \\
& 588107520G^2\delta^7B_{r,c_3} - 336061440B^2G^2\delta^7B_{r,c_3} + 318558240B^2G^2M\delta^7B_{r,c_3} + \\
& 220540320G^2\delta^8B_{r,c_3} - 80514720B^2G^2\delta^8B_{r,c_3} + 166280400B^2G^2M\delta^8B_{r,c_3} - \\
& 98017920G^2\delta^9B_{r,c_3} + 81681600B^2G^2\delta^9B_{r,c_3} - 9529520B^2G^2M\delta^9B_{r,c_3} - \\
& 127423296G^2\delta^{10}B_{r,c_3} + 71879808B^2G^2\delta^{10}B_{r,c_3} - 68612544B^2G^2M\delta^{10}B_{r,c_3} - \\
& 48117888G^2\delta^{11}B_{r,c_3} + 14257152B^2G^2\delta^{11}B_{r,c_3} - 36533952B^2G^2M\delta^{11}B_{r,c_3} - \\
& 6683040G^2\delta^{12}B_{r,c_3} - 6683040B^2G^2\delta^{12}B_{r,c_3} - 2598960B^2G^2M\delta^{12}B_{r,c_3} - \\
& 3769920B^2G^2\delta^{13}B_{r,c_3} + 4712400B^2G^2M\delta^{13}B_{r,c_3} - 538560B^2G^2\delta^{14}B_{r,c_3} + \\
& 1884960B^2G^2M\delta^{14}B_{r,c_3} + 233376B^2G^2M\delta^{15}B_{r,c_3} + 448975440G^2B_{r,c_4} + \\
& 370338778B^2G^2B_{r,c_4} - 319943349B^2G^2MB_{r,c_4} + 427567680G^2\delta B_{r,c_4} + \\
& 370019008B^2G^2\delta B_{r,c_4} - 319819635B^2G^2M\delta B_{r,c_4} - 110270160G^2\delta^2B_{r,c_4} - \\
& 294053760G^2\delta^3B_{r,c_4} - 477837360G^2\delta^4B_{r,c_4} - 18378360B^2G^2\delta^4B_{r,c_4} + \\
& 9189180B^2G^2M\delta^4B_{r,c_4} - 441080640G^2\delta^5B_{r,c_4} - 88216128B^2G^2\delta^5B_{r,c_4} + \\
& 49621572B^2G^2M\delta^5B_{r,c_4} - 110270160G^2\delta^6B_{r,c_4} - 200936736B^2G^2\delta^6B_{r,c_4} + \\
& 129873744B^2G^2M\delta^6B_{r,c_4} + 252046080G^2\delta^7B_{r,c_4} - 266048640B^2G^2\delta^7B_{r,c_4} + \\
& 204787440B^2G^2M\delta^7B_{r,c_4} + 330810480G^2\delta^8B_{r,c_4} - 202599540B^2G^2\delta^8B_{r,c_4} + \\
& 201068010B^2G^2M\delta^8B_{r,c_4} + 147026880G^2\delta^9B_{r,c_4} - 59899840B^2G^2\delta^9B_{r,c_4} + \\
& 108738630B^2G^2M\delta^9B_{r,c_4} - 36756720G^2\delta^{10}B_{r,c_4} + 38118080B^2G^2\delta^{10}B_{r,c_4} + \\
& 4900896B^2G^2M\delta^{10}B_{r,c_4} - 80196480G^2\delta^{11}B_{r,c_4} + 46335744B^2G^2\delta^{11}B_{r,c_4} - \\
& 38761632B^2G^2M\delta^{11}B_{r,c_4} - 43439760G^2\delta^{12}B_{r,c_4} + 16521960B^2G^2\delta^{12}B_{r,c_4} - \\
& 27567540B^2G^2M\delta^{12}B_{r,c_4} - 11309760G^2\delta^{13}B_{r,c_4} - 1256640B^2G^2\delta^{13}B_{r,c_4} - \\
& 6361740B^2G^2M\delta^{13}B_{r,c_4} - 1211760G^2\delta^{14}B_{r,c_4} - 2962080B^2G^2\delta^{14}B_{r,c_4} + \\
& 2019600B^2G^2M\delta^{14}B_{r,c_4} - 933504B^2G^2\delta^{15}B_{r,c_4} + 1750320B^2G^2M\delta^{15}B_{r,c_4} - \\
& 102102B^2G^2\delta^{16}B_{r,c_4} + 459459B^2G^2M\delta^{16}B_{r,c_4} + 45045B^2G^2M\delta^{17}B_{r,c_4}). \tag{53}
\end{aligned}$$

Adding Eq. (40) and Eq. (53) Our approximation's outcome up to the first component is

$$\begin{aligned}
\varphi_{OAFM} &= \frac{1+\delta}{2} + \frac{1}{225833287680B^2} (898646112G^2B_{r,c_3} + \\
& 510847008B^2G^2B_{r,c_3} - 432665232B^2G^2MB_{r,c_3} + \\
& 793054080G^2\delta B_{r,c_3} + 508540992B^2G^2\delta B_{r,c_3} - 431818768B^2G^2M\delta B_{r,c_3} - \\
& 441080640G^2\delta^2B_{r,c_3} - 882161280G^2\delta^3B_{r,c_3} - 955674720G^2\delta^4B_{r,c_3} - \\
& 73513440B^2G^2\delta^4B_{r,c_3} + 36756720B^2G^2M\delta^4B_{r,c_3} - 352864512G^2\delta^5B_{r,c_3} - \\
& 264648384B^2G^2\delta^5B_{r,c_3} + 154378224B^2G^2M\delta^5B_{r,c_3} + 411675264G^2\delta^6B_{r,c_3} - \\
& 421477056B^2G^2\delta^6B_{r,c_3} + 298954656B^2G^2M\delta^6B_{r,c_3} + 588107520G^2\delta^7B_{r,c_3} -
\end{aligned}$$

$$\begin{aligned}
 &336061440B^2G^2\delta^7B_{r,c_3} + 318558240B^2G^2M\delta^7B_{r,c_3} + 220540320G^2\delta^8B_{r,c_3} - \\
 &80514720B^2G^2\delta^8B_{r,c_3} + 166280400B^2G^2M\delta^8B_{r,c_3} - 98017920G^2\delta^9B_{r,c_3} + \\
 &81681600B^2G^2\delta^9B_{r,c_3} - 9529520B^2G^2M\delta^9B_{r,c_3} - 127423296G^2\delta^{10}B_{r,c_3} + \\
 &71879808B^2G^2\delta^{10}B_{r,c_3} - 68612544B^2G^2M\delta^{10}B_{r,c_3} - 48117888G^2\delta^{11}B_{r,c_3} + \\
 &14257152B^2G^2\delta^{11}B_{r,c_3} - 36533952B^2G^2M\delta^{11}B_{r,c_3} - 6683040G^2\delta^{12}B_{r,c_3} - \\
 &6683040B^2G^2\delta^{12}B_{r,c_3} - 2598960B^2G^2M\delta^{12}B_{r,c_3} - 3769920B^2G^2\delta^{13}B_{r,c_3} + \\
 &4712400B^2G^2M\delta^{13}B_{r,c_3} - 538560B^2G^2\delta^{14}B_{r,c_3} + 1884960B^2G^2M\delta^{14}B_{r,c_3} + \\
 &233376B^2G^2M\delta^{15}B_{r,c_3} + 448975440G^2B_{r,c_4} + 370338778B^2G^2B_{r,c_4} - \\
 &319943349B^2G^2MB_{r,c_4} + 427567680G^2\delta B_{r,c_4} + 370019008B^2G^2\delta B_{r,c_4} - \\
 &319819635B^2G^2M\delta B_{r,c_4} - 110270160G^2\delta^2B_{r,c_4} - 294053760G^2\delta^3B_{r,c_4} - \\
 &477837360G^2\delta^4B_{r,c_4} - 18378360B^2G^2\delta^4B_{r,c_4} + 9189180B^2G^2M\delta^4B_{r,c_4} - \\
 &441080640G^2\delta^5B_{r,c_4} - 88216128B^2G^2\delta^5B_{r,c_4} + 49621572B^2G^2M\delta^5B_{r,c_4} - \\
 &110270160G^2\delta^6B_{r,c_4} - 200936736B^2G^2\delta^6B_{r,c_4} + 129873744B^2G^2M\delta^6B_{r,c_4} + \\
 &252046080G^2\delta^7B_{r,c_4} - 266048640B^2G^2\delta^7B_{r,c_4} + 204787440B^2G^2M\delta^7B_{r,c_4} + \\
 &330810480G^2\delta^8B_{r,c_4} - 202599540B^2G^2\delta^8B_{r,c_4} + 201068010B^2G^2M\delta^8B_{r,c_4} + \\
 &147026880G^2\delta^9B_{r,c_4} - 59899840B^2G^2\delta^9B_{r,c_4} + 108738630B^2G^2M\delta^9B_{r,c_4} - \\
 &36756720G^2\delta^{10}B_{r,c_4} + 38118080B^2G^2\delta^{10}B_{r,c_4} + 4900896B^2G^2M\delta^{10}B_{r,c_4} - \\
 &80196480G^2\delta^{11}B_{r,c_4} + 46335744B^2G^2\delta^{11}B_{r,c_4} - 38761632B^2G^2M\delta^{11}B_{r,c_4} - \\
 &43439760G^2\delta^{12}B_{r,c_4} + 16521960B^2G^2\delta^{12}B_{r,c_4} - 27567540B^2G^2M\delta^{12}B_{r,c_4} - \\
 &11309760G^2\delta^{13}B_{r,c_4} - 1256640B^2G^2\delta^{13}B_{r,c_4} - 6361740B^2G^2M\delta^{13}B_{r,c_4} - \\
 &1211760G^2\delta^{14}B_{r,c_4} - 2962080B^2G^2\delta^{14}B_{r,c_4} + 2019600B^2G^2M\delta^{14}B_{r,c_4} - \\
 &933504B^2G^2\delta^{15}B_{r,c_4} + 1750320B^2G^2M\delta^{15}B_{r,c_4} - 102102B^2G^2\delta^{16}B_{r,c_4} + \\
 &459459B^2G^2M\delta^{16}B_{r,c_4} + 45045B^2G^2M\delta^{17}B_{r,c_4}). \tag{54}
 \end{aligned}$$

**7. Solution of the Problem Using Homotopy Analysis Method**

Solutions obtain from first iteration of velocity and temperature as given below,

$$\begin{aligned}
 v = &\frac{61}{720} B^2Gh - \frac{43B^2GhMx}{10080} - \frac{5}{48} B^2Gh\delta^2 + \frac{1}{160} B^2GhM\delta^3 + \frac{1}{48} B^2Ghx\delta^4 - \frac{1}{480} B^2GhM\delta^5 - \\
 &\frac{1}{720} B^2Gh\delta^6 + \frac{B^2GhM\delta^7}{10080} + \frac{1}{24} (5G - 6G\delta^2 + G\delta^4) + \frac{277Gh\Gamma}{8064} - \frac{61Gh\delta^2\Gamma}{1440} + \frac{5}{576} Gh\delta^4\Gamma - \\
 &\frac{Gh\delta^6\Gamma}{1440} + \frac{Ghy^8\Gamma}{40320}. \tag{55}
 \end{aligned}$$

$$\begin{aligned}
 \varphi = &-\frac{53BrG^2h}{3360} + \frac{53BrG^2hM}{6720} + \frac{809BrG^2hM\delta}{181440} + \frac{1}{48} BrG^2h\delta^4 - \frac{1}{96} BrG^2hM\delta^4 - \\
 &\frac{1}{160} BrG^2hM\delta^5 - \frac{1}{180} BrG^2h\delta^6 + \frac{1}{360} BrG^2hM\delta^6 + \frac{1}{504} BrG^2hM\delta^7 + \frac{BrG^2h\delta^8}{2016} -
 \end{aligned}$$

$$\frac{BrG^2hM\delta^8}{4032} - \frac{BrG^2hM\delta^9}{5184} + \frac{1+\delta}{2}. \quad (56)$$

Solutions obtain from second iteration of velocity and temperature as given below,

$$\begin{aligned} v = & -\frac{5Gh}{24} + \frac{61}{360}B^2Gh + \frac{61}{720}B^2Gh^2 + \frac{277B^4Gh^2}{8064} - \frac{2406463B^2BrG^3h^2M}{5448643200} - \\ & \frac{2329B^4Gh^2M^2}{14515200} + \frac{2406463B^2BrG^3h^2M^2}{10897286400} - \frac{43B^2GhM\delta}{5040} - \frac{43B^2Gh^2M\delta}{10080} - \frac{3973B^4Gh^2M\delta}{1814400} - \\ & \frac{453031B^2BrG^3h^2M^2\delta}{130767436800} + \frac{1}{4}Gh\delta^2 - \frac{5}{24}B^2Gh\delta^2 - \frac{5}{48}B^2Gh^2\delta^2 - \frac{61B^4Gh^2\delta^2}{1440} + \\ & \frac{3067B^2BrG^3h^2M\delta^2}{6652800} + \frac{73B^4Gh^2M^2\delta^2}{322560} - \frac{3067B^2BrG^3h^2M^2\delta^2}{13305600} + \frac{1}{80}B^2GhM\delta^3 + \\ & \frac{1}{160}B^2Gh^2M\delta^3 + \frac{11B^4Gh^2M\delta^3}{3360} + \frac{1403B^2BrG^3h^2M^2\delta^3}{80870400} - \frac{1}{24}Gh\delta^4 + \frac{1}{24}B^2Gh\delta^4 + \\ & \frac{1}{48}B^2Gh^2\delta^4 + \frac{5}{576}B^4Gh^2\delta^4 - \frac{43B^4Gh^2M^2\delta^4}{483840} - \frac{1}{240}B^2GhM\delta^5 - \frac{1}{480}B^2Gh^2M\delta^5 - \\ & \frac{17B^4Gh^2M\delta^5}{14400} - \frac{809B^2BrG^3h^2M^2\delta^5}{43545600} - \frac{1}{360}B^2Gh\delta^6 - \frac{1}{720}B^2Gh^2\delta^6 - \frac{B^4Gh^2\delta^6}{1440} + \\ & \frac{B^4Gh^2M^2\delta^6}{38400} + \frac{B^2GhM\delta^7}{5040} + \frac{B^2Gh^2M\delta^7}{10080} + \frac{B^4Gh^2M\delta^7}{10080} + \frac{809B^2BrG^3h^2M^2\delta^7}{914457600} + \\ & \frac{B^4Gh^2\delta^8}{40320} - \frac{B^2BrG^3h^2M\delta^8}{40320} - \frac{B^4Gh^2M^2\delta^8}{322560} + \frac{B^2BrG^3h^2M^2\delta^8}{80640} - \frac{B^4Gh^2M\delta^9}{362880} + \frac{B^2BrG^3h^2M^2\delta^9}{193536} + \\ & \frac{11B^2BrG^3h^2M\delta^{10}}{1814400} + \frac{B^4Gh^2M^2\delta^{10}}{14515200} - \frac{11B^2BrG^3h^2M^2\delta^{10}}{3628800} - \frac{7B^2BrG^3h^2M^2\delta^{11}}{4561920} - \\ & \frac{19B^2BrG^3h^2M\delta^{12}}{29937600} + \frac{19B^2BrG^3h^2M^2\delta^{12}}{59875200} + \frac{B^2BrG^3h^2M^2\delta^{13}}{5391360} + \frac{B^2BrG^3h^2M\delta^{14}}{36324288} - \\ & \frac{B^2BrG^3h^2M^2\delta^{14}}{72648576} - \frac{B^2BrG^3h^2M^2\delta^{15}}{113218560} + \frac{1}{24}(5G - 6G\delta^2 + G\delta^4) + \frac{277Gh\Gamma}{4032} + \frac{277Gh^2\Gamma}{8064} + \\ & \frac{50521B^2Gh^2\Gamma}{1814400} - \frac{90137B^2Gh^2M\delta\Gamma}{119750400} - \frac{61}{720}Gh\delta^2\Gamma - \frac{61Gh^2\delta^2\Gamma}{1440} - \frac{277B^2Gh^2\delta^2\Gamma}{8064} + \\ & \frac{12133B^2Gh^2M\delta^3\Gamma}{10886400} + \frac{5}{288}Gh\delta^4\Gamma + \frac{5}{576}Gh^2\delta^4\Gamma + \frac{61B^2Gh^2\delta^4\Gamma}{8640} - \frac{47B^2Gh^2M\delta^5\Gamma}{120960} - \\ & \frac{1}{720}Gh\delta^6\Gamma - \frac{Gh^2\delta^6\Gamma}{1440} - \frac{B^2Gh^2\delta^6\Gamma}{1728} + \frac{17B^2Gh^2M\delta^7\Gamma}{604800} + \frac{Gh\delta^8\Gamma}{20160} + \\ & \frac{Gh^2\delta^8\Gamma}{40320} + \frac{B^2Gh^2\delta^8\Gamma}{40320} - \frac{B^2Gh^2M\delta^9\Gamma}{725760} - \frac{B^2Gh^2\delta^{10}\Gamma}{1814400} + \frac{B^2Gh^2M\delta^{11}\Gamma}{39916800} + \\ & \frac{540553Gh^2\Gamma^2}{95800320} - \frac{50521Gh^2\delta^2\Gamma^2}{7257600} + \frac{277Gh^2\delta^4\Gamma^2}{193536} - \frac{61Gh^2\delta^6\Gamma^2}{518400} + \\ & \frac{Gh^2\delta^8\Gamma^2}{193536} - \frac{Gh^2\delta^{10}\Gamma^2}{7257600} + \frac{Gh^2\delta^{12}\Gamma^2}{479001600}. \end{aligned} \quad (57)$$

$$\begin{aligned}
\varphi = & -\frac{53BrG^2h}{1680} - \frac{53BrG^2h^2}{3360} - \frac{11687B^2BrG^2h^2}{907200} + \frac{53BrG^2hM}{3360} + \frac{53BrG^2h^2M}{6720} + \\
& \frac{11687B^2BrG^2h^2M}{1814400} - \frac{17324597Br^2G^4h^2M}{87178291200} - \frac{91B^2BrG^2h^2M^2}{2851200} + \frac{17324597Br^2G^4h^2M^2}{174356582400} + \\
& \frac{809BrG^2hM\delta}{90720} + \frac{809BrG^2h^2M\delta}{181440} + \frac{4471B^2BrG^2h^2M\delta}{1247400} + \frac{289B^2BrG^2h^2M^2\delta}{13305600} + \\
& \frac{2312301143Br^2G^4h^2M^2\delta}{80029671321600} + \frac{43B^2BrG^2h^2M\delta^3}{60480} - \frac{43B^2BrG^2h^2M^2\delta^3}{120960} + \frac{1}{24}BrG^2h\delta^4 + \\
& \frac{1}{48}BrG^2h^2\delta^4 + \frac{5}{288}B^2BrG^2h^2\delta^4 - \frac{1}{48}BrG^2hM\delta^4 - \frac{1}{96}BrG^2h^2M\delta^4 - \\
& \frac{5}{576}B^2BrG^2h^2M\delta^4 + \frac{53Br^2G^4h^2M\delta^4}{161280} - \frac{43B^2BrG^2h^2M^2\delta^4}{241920} - \frac{53Br^2G^4h^2M^2\delta^4}{322560} - \\
& \frac{1}{80}BrG^2hM\delta^5 - \frac{1}{160}BrG^2h^2M\delta^5 - \frac{47B^2BrG^2h^2M\delta^5}{7560} + \frac{61B^2BrG^2h^2M^2\delta^5}{120960} - \\
& \frac{809Br^2G^4h^2M^2\delta^5}{14515200} - \frac{1}{90}BrG^2h\delta^6 - \frac{1}{180}BrG^2h^2\delta^6 - \frac{11B^2BrG^2h^2\delta^6}{2160} + \frac{1}{180}BrG^2hM\delta^6 + \\
& \frac{1}{360}BrG^2h^2M\delta^6 + \frac{11B^2BrG^2h^2M\delta^6}{4320} - \frac{53Br^2G^4h^2M\delta^6}{604800} + \frac{61B^2BrG^2h^2M^2\delta^6}{181440} + \\
& \frac{53Br^2G^4h^2M^2\delta^6}{1209600} + \frac{1}{252}BrG^2hM\delta^7 + \frac{1}{504}BrG^2h^2M\delta^7 + \frac{67B^2BrG^2h^2M\delta^7}{30240} - \\
& \frac{B^2BrG^2h^2M^2\delta^7}{5040} + \frac{809Br^2G^4h^2M^2\delta^7}{45722880} + \frac{BrG^2h\delta^8}{1008} + \frac{BrG^2h^2\delta^8}{2016} + \frac{13B^2BrG^2h^2\delta^8}{20160} - \\
& \frac{BrG^2hM\delta^8}{2016} - \frac{BrG^2h^2M\delta^8}{4032} - \frac{13B^2BrG^2h^2M\delta^8}{40320} - \frac{577Br^2G^4h^2M\delta^8}{6773760} - \frac{B^2BrG^2h^2M^2\delta^8}{6720} + \\
& \frac{577Br^2G^4h^2M^2\delta^8}{13547520} - \frac{BrG^2hM\delta^9}{2592} - \frac{BrG^2h^2M\delta^9}{5184} - \frac{B^2BrG^2h^2M\delta^9}{3240} + \\
& \frac{B^2BrG^2h^2M^2\delta^9}{34560} + \frac{9397Br^2G^4h^2M^2\delta^9}{470292480} - \frac{B^2BrG^2h^2\delta^{10}}{32400} + \frac{B^2BrG^2h^2M\delta^{10}}{64800} + \\
& \frac{7Br^2G^4h^2M\delta^{10}}{129600} + \frac{B^2BrG^2h^2M^2\delta^{10}}{43200} - \frac{7Br^2G^4h^2M^2\delta^{10}}{259200} + \frac{7B^2BrG^2h^2M\delta^{11}}{475200} - \frac{B^2BrG^2h^2M^2\delta^{11}}{950400} + \\
& \frac{31Br^2G^4h^2M^2\delta^{11}}{2217600} - \frac{197Br^2G^4h^2M\delta^{12}}{15966720} - \frac{B^2BrG^2h^2M^2\delta^{12}}{1140480} + \frac{197Br^2G^4h^2M^2\delta^{12}}{31933440} + \\
& \frac{401Br^2G^4h^2M^2\delta^{13}}{113218560} + \frac{43Br^2G^4h^2M\delta^{14}}{33022080} - \frac{43Br^2G^4h^2M^2\delta^{14}}{66044160} - \frac{19Br^2G^4h^2M^2\delta^{15}}{45722880} - \\
& \frac{Br^2G^4h^2M\delta^{16}}{17418240} + \frac{Br^2G^4h^2M^2\delta^{16}}{34836480} + \frac{Br^2G^4h^2M^2\delta^{17}}{50761728} + \frac{1+\delta}{2} - \\
& \frac{10429BrG^2h^2\Gamma}{1995840} + \frac{10429BrG^2h^2M\Gamma}{3991680} + \frac{1144841BrG^2h^2M\delta\Gamma}{778377600} + \frac{61BrG^2h^2\delta^4\Gamma}{8640} - \\
& \frac{61BrG^2h^2M\delta^4\Gamma}{17280} - \frac{61BrG^2h^2M\delta^5\Gamma}{28800} - \frac{17BrG^2h^2\delta^6\Gamma}{8100} + \frac{17BrG^2h^2M\delta^6\Gamma}{16200} +
\end{aligned}$$

$$\begin{aligned} & \frac{17BrG^2h^2M\delta^7\Gamma}{22680} + \frac{17BrG^2h^2\delta^8\Gamma}{60480} - \frac{17BrG^2h^2M\delta^8\Gamma}{120960} - \frac{17BrG^2h^2M\delta^9\Gamma}{155520} \\ & \frac{BrG^2h^2\delta^{10}\Gamma}{56700} + \frac{BrG^2h^2M\delta^{10}\Gamma}{113400} + \frac{BrG^2h^2M\delta^{11}\Gamma}{138600} + \frac{BrG^2h^2\delta^{12}\Gamma}{1995840} - \\ & \frac{BrG^2h^2M\delta^{12}\Gamma}{3991680} - \frac{BrG^2h^2M\delta^{13}\Gamma}{4717440}. \end{aligned} \quad (58)$$

## 8. Flow Rate, Average Velocity and Shear Stress on the Plates

### 7.1 Flow Rate

The non-dimensional volume flux is given by

$$Q = \int_{-1}^1 v(\delta) d\delta, \quad (59)$$

substituting Eq. (47) in Eq. (59) we obtained

$$Q_{OAFM} = \frac{4G}{15} - \frac{29}{945} B^2 G c_1 + \frac{139B^2 G M c_1}{5670} - \frac{386G\Gamma c_1}{31185} - \frac{131B^2 G c_2}{10395} + \frac{56B^2 G M c_2}{4455} - \frac{2032G\Gamma c_2}{405405}. \quad (60)$$

Where  $c_1 = 10.043092231251727$ ,  $c_2 = -14.531897881927883$ .

Now substituting Eq. (55) in Eq. (59) we obtained

$$Q_{HAM} = \frac{4G}{15} + \frac{34}{315} B^2 G h + \frac{124Gh\Gamma}{2835}. \quad (61)$$

### 7.2 Average Velocity

The average velocity  $\tilde{v}$  is given by

$$\tilde{v} = \frac{Q}{S}. \quad (62)$$

Which in the non-dimensional form coincides with flow rate given in Eq. (60) and Eq. (61).

### 7.3 Shear Stress on the Upper Plate

The dimensionless share stress on the offer plates is given by

$$\tau = -\mu D[v, \delta], \delta = 1. \quad (63)$$

Here the minus sign accounts for the upper plate facing the negative  $y$ -direction of the coordinate system as shown in figure 1. Using Eq. (47) in Eq. (63) we obtained,

$$\tau_{OAFM} = \left\{ -\mu \left[ -\frac{G}{3} + \frac{\left( 1317888B^2 G c_1 - 1126400B^2 G M c_1 + 529408G\Gamma c_1 \right) + c_2 \left( 574464B^2 G - 603904B^2 G M c_2 + 227328G\Gamma c_2 \right)}{31933440} \right] \right\}. \quad (64)$$

Now using Eq. (55) in Eq. (63) we obtained

$$\tau_{HAM} = \left\{ -\mu \left( -\frac{G}{3} - \frac{2}{15} B^2 G h + \frac{1}{210} B^2 G h M - \frac{17Gh\Gamma}{315} \right) \right\}. \quad (65)$$

7.4 Shear Stress on the Lower Plate

Now the shear stress on the lower plate is calculated by the following formula

$$\tau = \mu D[v, \delta], \delta = -1, \tag{66}$$

using Eq. (47) in Eq. (66) we obtained,

$$\tau_{OAFM} = \left\{ -\mu \left[ \frac{G}{3} + \frac{\left( -1115136B^2Gc_1 + 850432B^2GMc_1 - 450560G\Gamma c_1 - 439296B^2Gc_2 + 426752B^2GMc_2 - 175104G\Gamma c_2 \right)}{31933440} \right] \right\}. \tag{67}$$

Now, using Eq. (55) in Eq. (66) we obtained

$$\tau_{HAM} = \left\{ -\mu \left( \frac{G}{3} + \frac{2}{15} B^2 Gh + \frac{1}{210} B^2 GhM + \frac{17Gh\Gamma}{315} \right) \right\}. \tag{68}$$

**Table 1:** Residual error of OAFM and HAM solutions for velocity when  $\Gamma=0.02$ ,  $G=0.0001$ ,  $B=0.003$ ,  $M=0.0005$ ,  $B_r = 0.001$ .

y	OAFM Solution $U$	Residual $R(U)$	HAM Solution $U$	Residual $R(U)$	Average Residual
-1.	$-1.69718 \times 10^{-21}$	$-1.67243 \times 10^{-7}$	$1.06228 \times 10^{-21}$	-0.0001	$-3.50836 \times 10^{-5}$
-0.9	$3.30471 \times 10^{-6}$	$-9.55272 \times 10^{-8}$	$3.2319 \times 10^{-8}$	$-9.97999 \times 10^{-5}$	$-3.49748 \times 10^{-5}$
-0.8	$6.51552 \times 10^{-6}$	$-2.22832 \times 10^{-8}$	$6.38413 \times 10^{-8}$	$-9.96054 \times 10^{-5}$	$-3.48672 \times 10^{-5}$
-0.7	$9.54769 \times 10^{-6}$	$4.07313 \times 10^{-8}$	$9.37898 \times 10^{-8}$	$-9.94218 \times 10^{-5}$	$-3.47688 \times 10^{-5}$
-0.6	$1.23265 \times 10^{-5}$	$8.48947 \times 10^{-8}$	$1.21427 \times 10^{-7}$	$-9.92535 \times 10^{-5}$	$-3.46853 \times 10^{-5}$
-0.5	$1.47872 \times 10^{-5}$	$1.05704 \times 10^{-7}$	$1.46072 \times 10^{-7}$	$-9.91045 \times 10^{-5}$	$-3.46205 \times 10^{-5}$
-0.4	$1.6875 \times 10^{-5}$	$1.03267 \times 10^{-7}$	$1.67119 \times 10^{-7}$	$-9.8978 \times 10^{-5}$	$-3.45756 \times 10^{-5}$
-0.3	$1.85452 \times 10^{-5}$	$8.211 \times 10^{-8}$	$1.8405 \times 10^{-7}$	$-9.88768 \times 10^{-5}$	$-3.45493 \times 10^{-5}$
-0.2	$1.9763 \times 10^{-5}$	$5.00582 \times 10^{-8}$	$1.9645 \times 10^{-7}$	$-9.88031 \times 10^{-5}$	$-3.45384 \times 10^{-5}$
-0.1	$2.05035 \times 10^{-5}$	$1.61669 \times 10^{-8}$	$2.04014 \times 10^{-7}$	$-9.87582 \times 10^{-5}$	$-3.4539 \times 10^{-5}$
0.	$2.07518 \times 10^{-5}$	$-1.19245 \times 10^{-8}$	$2.06556 \times 10^{-7}$	$-9.87431 \times 10^{-5}$	$-3.45476 \times 10^{-5}$
0.1	$2.05031 \times 10^{-5}$	$-3.02603 \times 10^{-8}$	$2.04014 \times 10^{-7}$	$-9.87582 \times 10^{-5}$	$-3.45622 \times 10^{-5}$
0.2	$1.97623 \times 10^{-5}$	$-3.91934 \times 10^{-8}$	$1.9645 \times 10^{-7}$	$-9.88031 \times 10^{-5}$	$-3.45831 \times 10^{-5}$
0.3	$1.85443 \times 10^{-5}$	$-4.14701 \times 10^{-8}$	$1.8405 \times 10^{-7}$	$-9.88768 \times 10^{-5}$	$-3.46111 \times 10^{-5}$
0.4	$1.6874 \times 10^{-5}$	$-3.82653 \times 10^{-8}$	$1.67119 \times 10^{-7}$	$-9.8978 \times 10^{-5}$	$-3.46464 \times 10^{-5}$
0.5	$1.47862 \times 10^{-5}$	$-2.58484 \times 10^{-8}$	$1.46072 \times 10^{-7}$	$-9.91045 \times 10^{-5}$	$-3.46863 \times 10^{-5}$
0.6	$1.23257 \times 10^{-5}$	$2.4856 \times 10^{-9}$	$1.21427 \times 10^{-7}$	$-9.92535 \times 10^{-5}$	$-3.47265 \times 10^{-5}$
0.7	$9.54705 \times 10^{-6}$	$4.49492 \times 10^{-8}$	$9.37898 \times 10^{-8}$	$-9.94218 \times 10^{-5}$	$-3.47666 \times 10^{-5}$
0.8	$6.5151 \times 10^{-6}$	$7.13306 \times 10^{-8}$	$6.38413 \times 10^{-8}$	$-9.96054 \times 10^{-5}$	$-3.48204 \times 10^{-5}$
0.9	$3.3045 \times 10^{-6}$	$7.8733 \times 10^{-9}$	$3.2319 \times 10^{-8}$	$-9.97999 \times 10^{-5}$	$-3.49231 \times 10^{-5}$
1.	$-1.71552 \times 10^{-21}$	$-2.42568 \times 10^{-7}$	$1.3722 \times 10^{-21}$	-0.0001	$-3.51213 \times 10^{-5}$

**Table 2:** Residual error of OAFM and HAM solutions for temperature when  $\Gamma=0.02$ ,  $G=0.0001$ ,  $B=0.003$ ,  $M=0.0005$ ,  $B_r = 0.001$ .

y	OAFM Solution $\varphi$	Residual R ( $\varphi$ )	HAM Solution ( $\varphi$ )	Residual R ( $\varphi$ )	Average Residual
-1.	$6.82794 \times 10^{-23}$	$4.15076 \times 10^{-12}$	$-4.89094 \times 10^{-29}$	$1.11122 \times 10^{-12}$	$2.63099 \times 10^{-12}$
-0.9	0.05	$2.01263 \times 10^{-8}$	0.05	$1.78754 \times 10^{-12}$	$1.0064 \times 10^{-8}$
-0.8	0.1	$7.46622 \times 10^{-8}$	0.1	$3.75338 \times 10^{-12}$	$3.7333 \times 10^{-8}$
-0.7	0.15	$1.55612 \times 10^{-7}$	0.15	$6.81879 \times 10^{-12}$	$7.78095 \times 10^{-8}$
-0.6	0.2	$2.56275 \times 10^{-7}$	0.2	$1.06841 \times 10^{-11}$	$1.28143 \times 10^{-7}$
-0.5	0.25	$3.71395 \times 10^{-7}$	0.25	$1.49701 \times 10^{-11}$	$1.85705 \times 10^{-7}$
-0.4	0.3	$4.96806 \times 10^{-7}$	0.3	$1.92563 \times 10^{-11}$	$2.48413 \times 10^{-7}$
-0.3	0.35	$6.28535 \times 10^{-7}$	0.35	$2.31225 \times 10^{-11}$	$3.14279 \times 10^{-7}$
-0.2	0.4	$7.61599 \times 10^{-7}$	0.4	$2.61903 \times 10^{-11}$	$3.80812 \times 10^{-7}$
-0.1	0.45	$8.88884 \times 10^{-7}$	0.45	$2.81596 \times 10^{-11}$	$4.44456 \times 10^{-7}$
0.	0.5	$1.00049 \times 10^{-6}$	0.5	$2.88381 \times 10^{-11}$	$5.0026 \times 10^{-7}$
0.1	0.55	$1.08381 \times 10^{-6}$	0.55	$2.81596 \times 10^{-11}$	$5.41917 \times 10^{-7}$
0.2	0.6	$1.12449 \times 10^{-6}$	0.6	$2.61903 \times 10^{-11}$	$5.62261 \times 10^{-7}$
0.3	0.65	$1.10859 \times 10^{-6}$	0.65	$2.31225 \times 10^{-11}$	$5.54308 \times 10^{-7}$
0.4	0.7	$1.02592 \times 10^{-6}$	0.7	$1.92562 \times 10^{-11}$	$5.12969 \times 10^{-7}$
0.5	0.75	$8.74798 \times 10^{-7}$	0.75	$1.49699 \times 10^{-11}$	$4.37407 \times 10^{-7}$
0.6	0.8	$6.67273 \times 10^{-7}$	0.8	$1.06839 \times 10^{-11}$	$3.33642 \times 10^{-7}$
0.7	0.85	$4.32393 \times 10^{-7}$	0.85	$6.81849 \times 10^{-12}$	$2.162 \times 10^{-7}$
0.8	0.9	$2.13674 \times 10^{-7}$	0.9	$3.75298 \times 10^{-12}$	$1.06839 \times 10^{-7}$
0.9	0.95	$5.78024 \times 10^{-8}$	0.95	$1.78705 \times 10^{-12}$	$2.89021 \times 10^{-8}$
1.	1.	$-1.33663 \times 10^{-12}$	1.	$1.11066 \times 10^{-12}$	$-1.12983 \times 10^{-13}$

## 9. Numerical Results and Discussions

In this paper we successfully implemented the Optimal Auxiliary Function Method (OAFM) and Homotopy Analysis Method (HAM) to analyze the inclined flow of couple stress fluid under the influence of MHD. Several parameters were studied in relation to velocity profile and temperature distribution. Figures (2) and (3) are plotted to see the effect of MHD parameter  $\Gamma$  on velocity profile Using OAFM and HAM. In this study, we found an inverse relationship between parameter  $\Gamma$  and velocity profile. Figures (4) and (5) show that as we increase the parameter B the graph of velocity profile is also increases. Figures (6) and (7) show the direct relation between parameter G and velocity. Figures (8-11) shows the effect of different parameters M and Br on temperature distribution using OAFM and HAM solution The non-dimensional parameter Br stands for the Brinkman number, which is directly relation to the temperature distribution. Figures (12-15) show the effect of shear stress on the upper plate against different parameters by using OAFM and HAM solutions. Figures (16-19) show the behaviour of shear stress on the lower plate against different parameters in the OAFM and HAM solutions. The flow rate is shown in Figures (20) and (21) for various parameters of the OAFM and HAM solutions. Tables 1 and 2 show the solutions for the velocity profile and temperature distributions, as well as their residual error and average residual using the OAFM and HAM solutions. The following tables illustrate a comparison of the results of the two methods for varying values of the independent variable y and the parameters G, M, B, and  $\Gamma$ . Tables 3 and 4 show the velocity profile and temperature distribution as well as the absolute difference between them for various parameter values.

**Table 3:** Absolute difference for velocity field  $u$  on both OAFM and HAM technique, keeping  $\Gamma=0.02$ ,  $G=0.0001$ ,  $B=0.003$ ,  $M=0.0005$ ,  $B_r = 0.001$ .

Y	OAFM Solution $U$	HAM Solution $U$	Absolute difference
-1.	$-1.69718 \times 10^{-21}$	$1.06228 \times 10^{-21}$	$2.19651 \times 10^{-21}$
-0.9	$3.30471 \times 10^{-6}$	$3.2319 \times 10^{-8}$	$2.28923 \times 10^{-6}$
-0.8	$6.51552 \times 10^{-6}$	$6.38413 \times 10^{-8}$	$4.51331 \times 10^{-6}$
-0.7	$9.54769 \times 10^{-6}$	$9.37898 \times 10^{-8}$	$6.6135 \times 10^{-6}$
-0.6	$1.23265 \times 10^{-5}$	$1.21427 \times 10^{-7}$	$8.53801 \times 10^{-6}$
-0.5	$1.47872 \times 10^{-5}$	$1.46072 \times 10^{-7}$	$1.02421 \times 10^{-5}$
-0.4	$1.6875 \times 10^{-5}$	$1.67119 \times 10^{-7}$	$1.16877 \times 10^{-5}$
-0.3	$1.85452 \times 10^{-5}$	$1.8405 \times 10^{-7}$	$1.28441 \times 10^{-5}$
-0.2	$1.9763 \times 10^{-5}$	$1.9645 \times 10^{-7}$	$1.36872 \times 10^{-5}$
-0.1	$2.05035 \times 10^{-5}$	$2.04014 \times 10^{-7}$	$1.41998 \times 10^{-5}$
0.	$2.07518 \times 10^{-5}$	$2.06556 \times 10^{-7}$	$1.43717 \times 10^{-5}$
0.1	$2.05031 \times 10^{-5}$	$2.04014 \times 10^{-7}$	$1.41995 \times 10^{-5}$
0.2	$1.97623 \times 10^{-5}$	$1.9645 \times 10^{-7}$	$1.36866 \times 10^{-5}$
0.3	$1.85443 \times 10^{-5}$	$1.8405 \times 10^{-7}$	$1.28433 \times 10^{-5}$
0.4	$1.6874 \times 10^{-5}$	$1.67119 \times 10^{-7}$	$1.16868 \times 10^{-5}$
0.5	$1.47862 \times 10^{-5}$	$1.46072 \times 10^{-7}$	$1.02411 \times 10^{-5}$
0.6	$1.23257 \times 10^{-5}$	$1.21427 \times 10^{-7}$	$8.53719 \times 10^{-6}$
0.7	$9.54705 \times 10^{-6}$	$9.37898 \times 10^{-8}$	$6.61286 \times 10^{-6}$
0.8	$6.5151 \times 10^{-6}$	$6.38413 \times 10^{-8}$	$4.51289 \times 10^{-6}$
0.9	$3.3045 \times 10^{-6}$	$3.2319 \times 10^{-8}$	$2.28902 \times 10^{-6}$
1.	$-1.71552 \times 10^{-21}$	$-1.37221 \times 10^{-21}$	$2.03175 \times 10^{-21}$

## 10. Conclusion

In this study, employing the Reynolds viscosity model between two parallel inclined plates with no slip boundary conditions, we investigate the impact of MHD on couple stress fluid. The governing equations of a couple stress fluids under the influence of MHD is solved using the Optimal Auxiliary Function Method (OAFM) and Homotopy Analysis Method (HAM). For resolving nonlinear differential equations involving velocity profile, energy distribution, volume flux, flow rate, and shear stresses on both plates, the Homotopy Analysis Method (HAM) is an analytical technique, and the Optimal Auxiliary Function Method (OAFM) is a numerical technique. On the graphical representation, we can see that flow rate, average velocity, shear stress, and dimensionless parameters  $G$ ,  $B$ ,  $M$ , and  $Br$  are strongly correlated.

**Table 4:** Absolute difference for temperature on both OAFM and HAM technique, keeping  $\Gamma=0.02$ ,  $G=0.0001$ ,  $B=0.003$ ,  $M=0.0005$ ,  $B_r = 0.001$ .

$y$	OAFM Solution $\varphi$	HAM Solution $\varphi$	Absolute difference
-1	$6.82794 \times 10^{-23}$	$-4.89094 \times 10^{-29}$	$4.77956 \times 10^{-23}$
-0.9	0.05	0.05	$1.0819 \times 10^{-8}$
-0.8	0.1	0.1	$2.1638 \times 10^{-8}$
-0.7	0.15	0.15	$3.24569 \times 10^{-8}$
-0.6	0.2	0.2	$4.32753 \times 10^{-8}$
-0.5	0.25	0.25	$5.40902 \times 10^{-8}$
-0.4	0.3	0.3	$6.48883 \times 10^{-8}$
-0.3	0.35	0.35	$7.56279 \times 10^{-8}$
-0.2	0.4	0.4	$8.62047 \times 10^{-8}$
-0.1	0.45	0.45	$9.63988 \times 10^{-8}$
0.	0.5	0.5	$1.05812 \times 10^{-7}$
0.1	0.55	0.55	$1.13808 \times 10^{-7}$
0.2	0.6	0.6	$1.19496 \times 10^{-7}$
0.3	0.65	0.65	$1.21772 \times 10^{-7}$
0.4	0.7	0.7	$1.19473 \times 10^{-7}$
0.5	0.75	0.75	$1.11625 \times 10^{-7}$
0.6	0.8	0.8	$9.77637 \times 10^{-8}$
0.7	0.85	0.85	$7.8215 \times 10^{-8}$
0.8	0.9	0.9	$5.41935 \times 10^{-8}$
0.9	0.95	0.95	$2.75367 \times 10^{-8}$
1.	1.	1.	0.

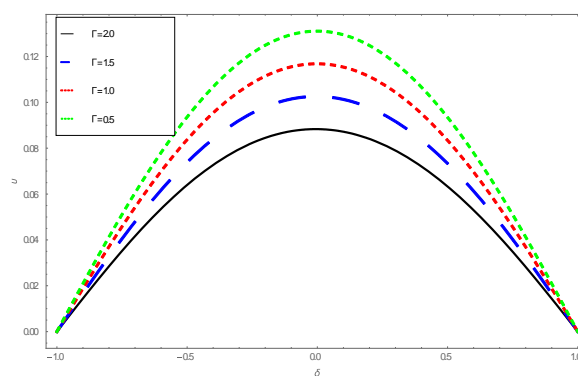


**Figure 2:** Velocity profile against parameter  $\Gamma$  using OAFM.

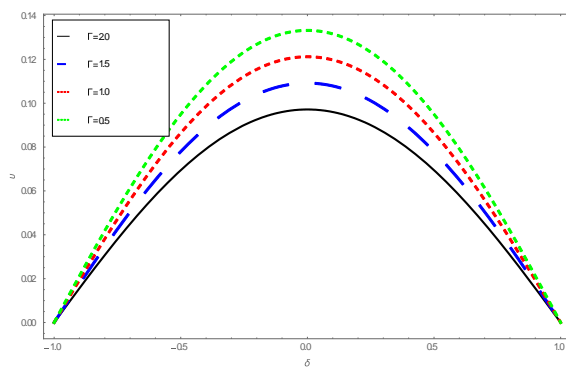


**Figure 3:** Velocity profile against parameter  $\Gamma$  using HAM.

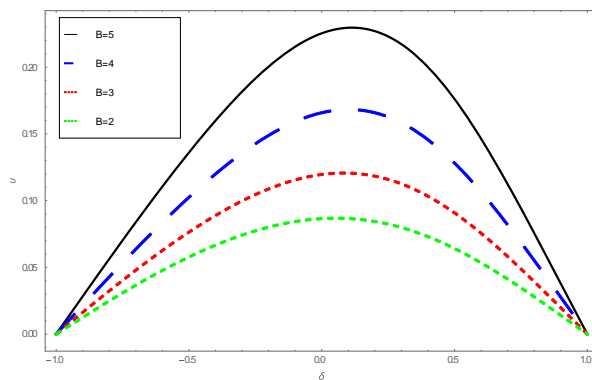


**Figure 4:** Velocity profile against parameter  $B$  using OAFM.

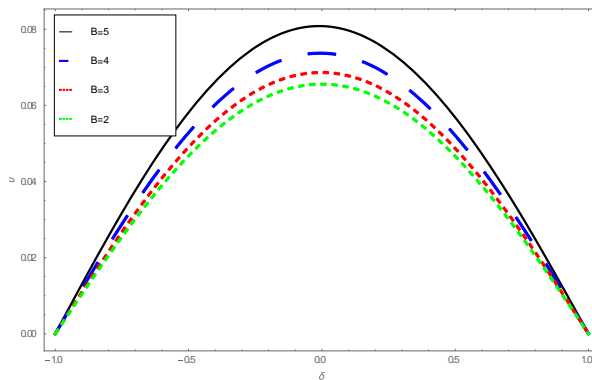


**Figure 5:** Velocity profile against parameter  $B$  using HAM.

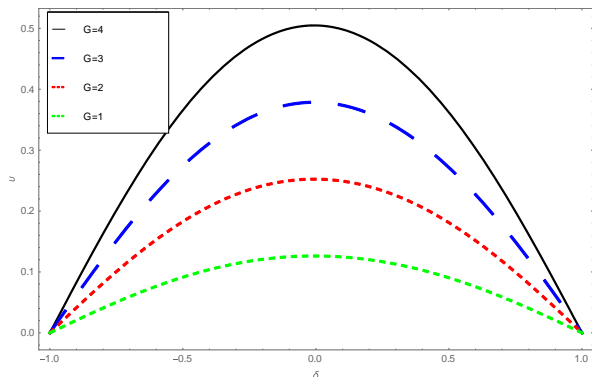


**Figure 6:** Velocity profile against parameter  $G$  using OAFM.

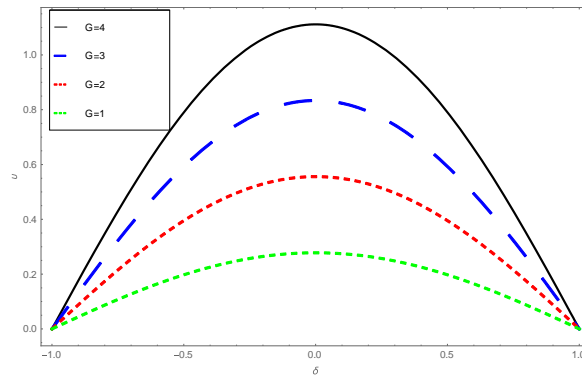


**Figure 7:** Velocity profile against parameter  $G$  using HAM.

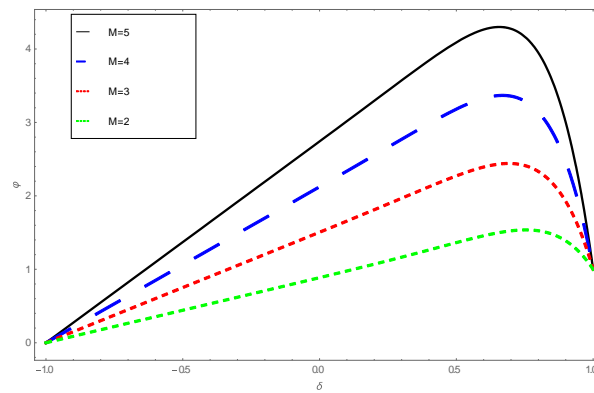


**Figure 8:** Temperature profile against parameter  $M$  using OAFM.

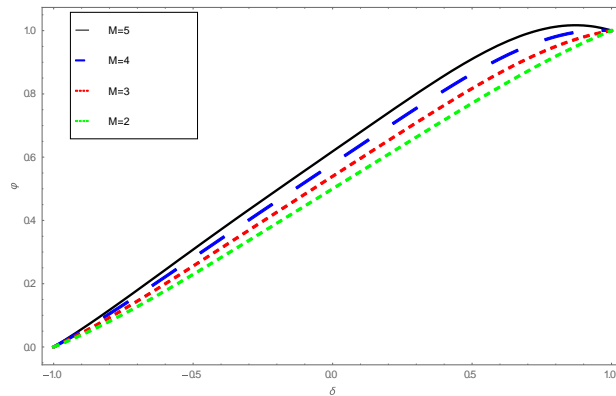


**Figure 9:** Temperature profile against parameter  $M$  using HAM.

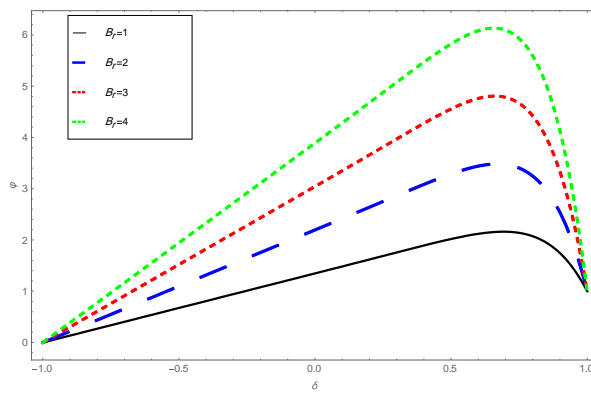


**Figure 10:** Temperature profile against parameter  $B_r$  using OAFM.

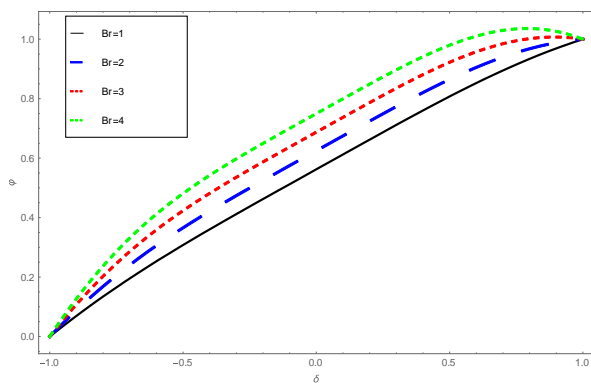


**Figure 11:** Temperature profile against parameter  $B_r$  using HAM.

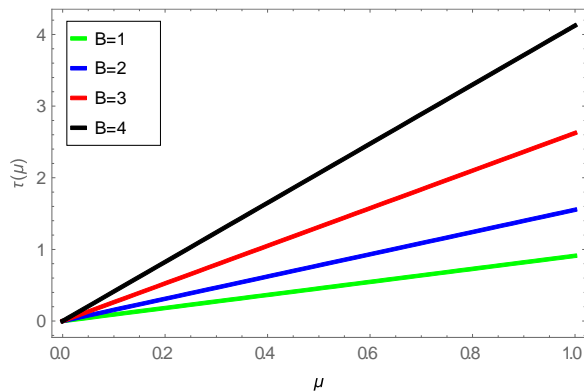


**Figure 12:** Shear stress on upper plate against parameter  $B$  at  $G = 2$  and  $M = 3$  using OAFM.

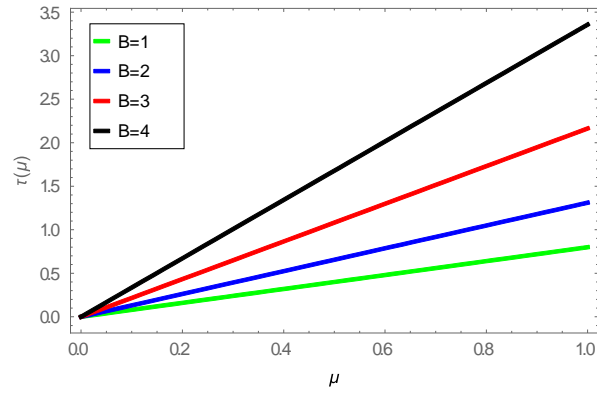


**Figure 13:** Shear stress on upper plate against parameter  $B$  at  $G = 2$  and  $M = 3$  using HAM.

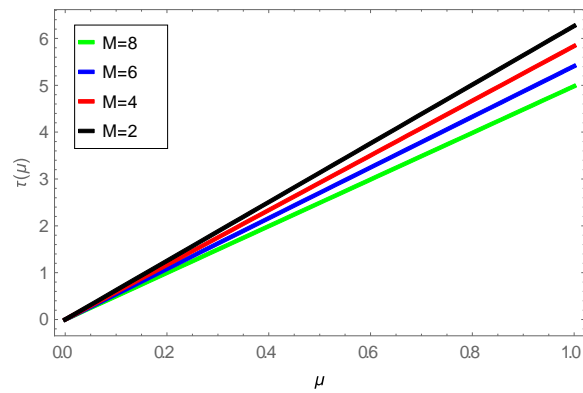


**Figure 14:** Shear stress on upper plate against parameter  $M$  at  $G = 2$  and  $B = 5$  using OAFM.

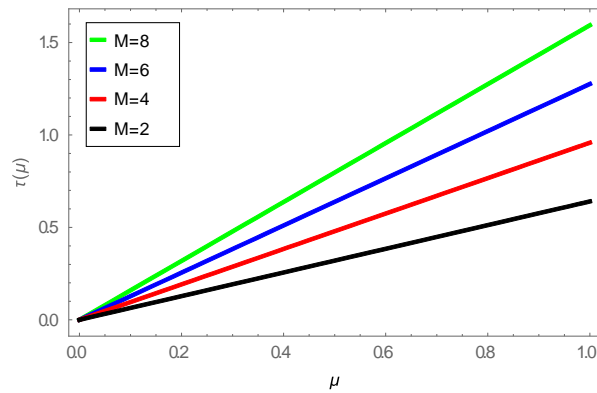


**Figure 15:** Shear stress on upper plate against parameter  $M$  at  $G = 2$  and  $B = 5$  using HAM.

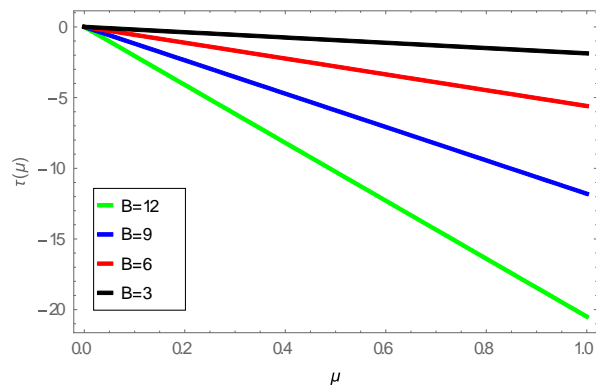


**Figure 16:** Shear stress on lower plate against parameter B keeping  $G = 2$  and  $M = 3$  using OAFM.

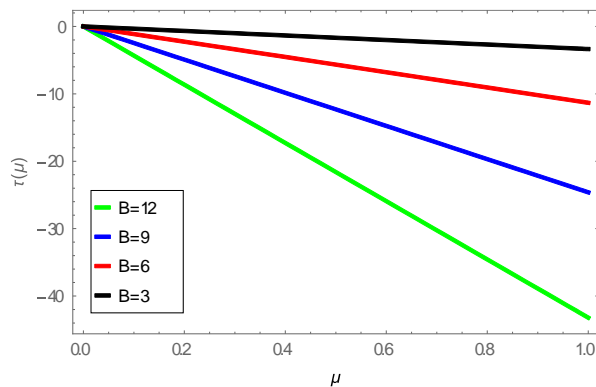


**Figure 17:** Shear stress on lower plate against parameter B keeping  $G = 2$  and  $M = 3$  using HAM.

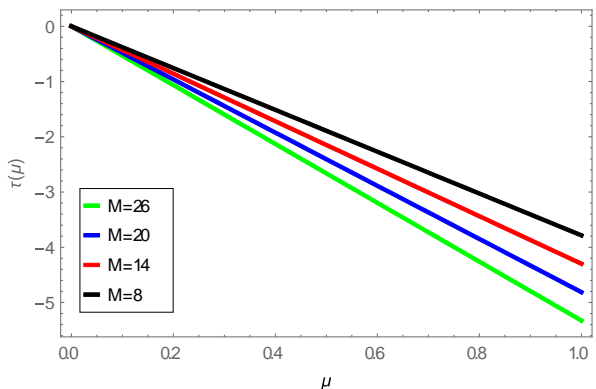


**Figure 18:** Shear stress on lower plate against parameter M keeping  $G = 2$  and  $B = 3$  using OAFM.

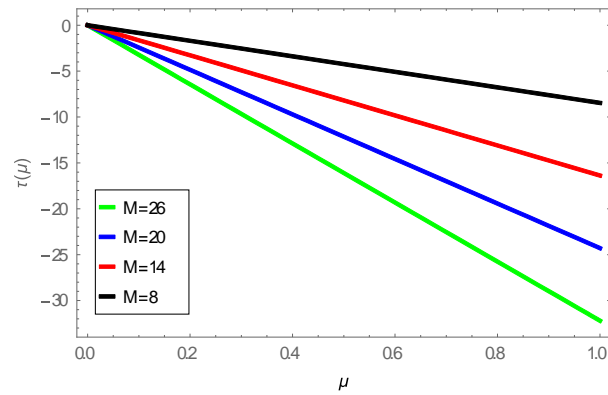


**Figure 19:** Shear stress on lower plate against parameter  $M$  keeping  $G = 2$  and  $B = 3$  using HAM.

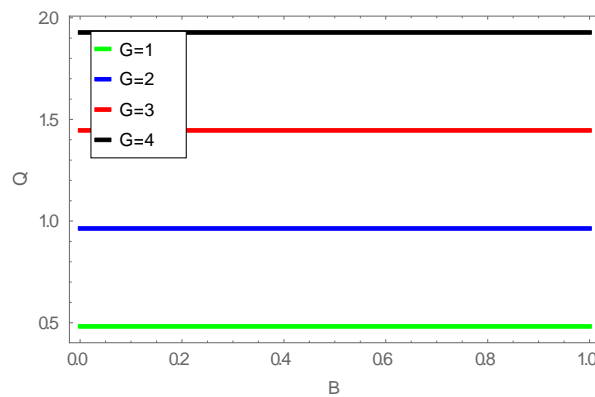


**Figure 20:** Flow rate for different values of  $G$  when  $B = 1$  and  $M = 4$  using OAFM.

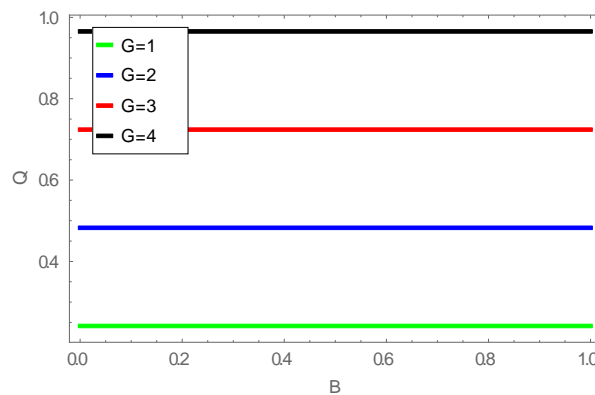


**Figure 21:** Flow rate for different values of  $G$  when  $B = 1$  and  $M = 4$  using HAM.

## References

- [1] R. N. Kumar, R. P. Gowda, A. M. Abusorrah, Y. Mahrous, N. H. Abu-Hamdeh, A. Issakhov, M. Rahimi-Gorji, B. Prasannakumara, Impact of magnetic dipole on ferromagnetic hybrid nanofluid flow over a stretching cylinder, *Physica Scripta*, Vol. 96, No. 4, pp. 045215, 2021.
- [2] R. P. Gowda, R. N. Kumar, A. Rauf, B. Prasannakumara, S. Shehzad, Magnetized flow of sutterby nanofluid through cattaneo-christov theory of heat diffusion and stefan blowing condition, *Applied Nanoscience*, Vol. 13, No. 1, pp. 585-594, 2023.
- [3] R. P. Gowda, R. N. Kumar, B. Prasannakumara, B. Nagaraja, B. Gireesha, Exploring magnetic dipole contribution on ferromagnetic nanofluid flow over a stretching sheet: An application of Stefan blowing, *Journal of Molecular Liquids*, Vol. 335, pp. 116215, 2021.

- [4] T. A. Yusuf, F. Mabood, B. Prasannakumara, I. E. Sarris, Magneto-bioconvection flow of Williamson nanofluid over an inclined plate with gyrotactic microorganisms and entropy generation, *Fluids*, Vol. 6, No. 3, pp. 109, 2021.
- [5] R. N. Kumar, A. Jyothi, H. Alhumade, R. P. Gowda, M. M. Alam, I. Ahmad, M. Gorji, B. Prasannakumara, Impact of magnetic dipole on thermophoretic particle deposition in the flow of Maxwell fluid over a stretching sheet, *Journal of Molecular Liquids*, Vol. 334, pp. 116494, 2021.
- [6] G. Domairry, M. Hatami, Squeezing Cu–water nanofluid flow analysis between parallel plates by DTM-Padé Method, *Journal of Molecular Liquids*, Vol. 193, pp. 37-44, 2014.
- [7] O. Pourmehran, M. Rahimi-Gorji, M. Gorji-Bandpy, D. Ganji, RETRACTED: analytical investigation of squeezing unsteady nanofluid flow between parallel plates by LSM and CM, Elsevier, 2015.
- [8] U. Khan, N. Ahmed, M. Asadullah, S. T. Mohyud-din, Effects of viscous dissipation and slip velocity on two-dimensional and axisymmetric squeezing flow of Cu-water and Cu-kerosene nanofluids, *Propulsion and Power research*, Vol. 4, No. 1, pp. 40-49, 2015.
- [9] H. Alfvén, Existence of electromagnetic-hydrodynamic waves, *Nature*, Vol. 150, No. 3805, pp. 405-406, 1942.
- [10] N. T. EL-Dabe, S. M. El-Mohandis, Effect of couple stresses on pulsatile hydromagnetic Poiseuille flow, *Fluid Dynamics Research*, Vol. 15, No. 5, pp. 313-324, 1995.
- [11] M. Farooq, S. Islam, M. Rahim, A. Siddiqui, Laminar flow of couple stress fluids for Vogel's model, *Sci. Res. Essays*, Vol. 7, No. 33, pp. 2936-2961, 2012.
- [12] W. Manyonge, D. Kiema, C. Iyaya, Steady MHD poiseuille flow between two infinite parallel porous plates in an inclined magnetic field, *International journal of pure and applied mathematics*, Vol. 76, No. 5, pp. 661-668, 2012.
- [13] N. Herisanu, V. Marinca, An efficient analytical approach to investigate the dynamics of a misaligned multirotor system, *Mathematics*, Vol. 8, No. 7, pp. 1083, 2020.
- [14] N. Herisanu, V. Marinca, G. Madescu, F. Dragan, Dynamic response of a permanent magnet synchronous generator to a wind gust, *Energies*, Vol. 12, No. 5, pp. 915, 2019.
- [15] V. Marinca, N. Herisanu, An application of the optimal auxiliary functions to Blasius problem, *The Romanian Journal of Technical Sciences. Applied Mechanics.*, Vol. 60, No. 3, pp. 206-215, 2015.
- [16] V. Marinca, B. Marinca, Optimal auxiliary functions method for nonlinear thin film flow of a third grade fluid on a moving belt, *A A*, Vol. 2, No. 2, pp. 1-2, 2018.
- [17] V. Marinca, R.-D. Ene, V. B. Marinca, Optimal Auxiliary Functions Method for viscous flow due to a stretching surface with partial slip, *Open Engineering*, Vol. 8, No. 1, pp. 261-274, 2018.
- [18] V. Marinca, N. Herisanu, Optimal auxiliary functions method for a pendulum wrapping on two cylinders, *Mathematics*, Vol. 8, No. 8, pp. 1364, 2020.
- [19] L. Zada, R. Nawaz, M. Ayaz, H. Ahmad, H. Alrabaiah, Y.-M. Chu, New algorithm for the approximate solution of generalized seventh order Korteweg-Devries equation arising in shallow water waves, *Results in Physics*, Vol. 20, pp. 103744, 2021.
- [20] S. Liao, Comparison between the homotopy analysis method and homotopy perturbation method, *Applied Mathematics and Computation*, Vol. 169, No. 2, pp. 1186-1194, 2005.
- [21] D. Srinivasacharya, K. Kaladhar, Mixed convection flow of couple stress fluid between parallel vertical plates with Hall and Ion-slip effects, *Communications in Nonlinear Science and Numerical Simulation*, Vol. 17, No. 6, pp. 2447-2462, 2012.
- [22] D. Srinivasacharya, K. Kaladhar, Mixed convection flow of chemically reacting couple stress fluid in a vertical channel with Soret and Dufour effects, *International Journal for Computational Methods in Engineering Science and Mechanics*, Vol. 15, No. 5, pp. 413-421, 2014.
- [23] M. Ramzan, M. Farooq, A. Alsaedi, T. Hayat, MHD three-dimensional flow of couple stress fluid with Newtonian heating, *The European Physical Journal Plus*, Vol. 128, pp. 1-15, 2013.
- [24] N. A. Khan, S. Aziz, N. A. Khan, Numerical simulation for the unsteady MHD flow and heat transfer of couple stress fluid over a rotating disk, *Plos One*, Vol. 9, No. 5, pp. e95423, 2014.
- [25] T. Hayat, A. Aziz, T. Muhammad, B. Ahmad, Influence of magnetic field in three-dimensional flow of couple stress nanofluid over a nonlinearly stretching surface with convective condition, *PloS one*, Vol. 10, No. 12, pp. e0145332, 2015.
- [26] M. Ramzan, Influence of Newtonian heating on three dimensional MHD flow of couple stress nanofluid with viscous dissipation and joule heating, *PloS one*, Vol. 10, No. 4, pp. e0124699, 2015.
- [27] T. Hayat, T. Muhammad, S. A. Shehzad, A. Alsaedi, Simultaneous effects of magnetic field and convective condition in three-dimensional flow of couple stress nanofluid with heat generation/absorption, *Journal of the Brazilian Society of Mechanical Sciences and Engineering*, Vol. 39, pp. 1165-1176, 2017.

- [28] F. Awad, N. Haroun, P. Sibanda, M. Khumalo, On couple stress effects on unsteady nanofluid flow over stretching surfaces with vanishing nanoparticle flux at the wall, *Journal of Applied Fluid Mechanics*, Vol. 9, No. 4, pp. 1937-1944, 2016.
- [29] T. Hayat, M. Awais, A. Safdar, A. A. Hendi, Unsteady three dimensional flow of couple stress fluid over a stretching surface with chemical reaction, *Nonlinear Analysis: Modelling and Control*, Vol. 17, No. 1, pp. 47-59, 2012.
- [30] A. R. Hadjesfandiari, G. F. Dargush, Couple stress theories: Theoretical underpinnings and practical aspects from a new energy perspective, *arXiv preprint arXiv:1611.10249*, 2016.
- [31] D. Tripathi, Peristaltic hemodynamic flow of couple-stress fluids through a porous medium with slip effect, *Transport in porous media*, Vol. 92, pp. 559-572, 2012.
- [32] M. Devakar, D. Sreenivasu, B. Shankar, Analytical solutions of couple stress fluid flows with slip boundary conditions, *Alexandria Engineering Journal*, Vol. 53, No. 3, pp. 723-730, 2014.
- [33] G. Ramanaiah, Squeeze films between finite plates lubricated by fluids with couple stress, *Wear*, Vol. 54, No. 2, pp. 315-320, 1979.
- [34] S. Chippa, M. Sarangi, Elastohydrodynamically lubricated finite line contact with couple stress fluids, *Tribology International*, Vol. 67, pp. 11-20, 2013.
- [35] A. Alsaedi, N. Ali, D. Tripathi, T. Hayat, Peristaltic flow of couple stress fluid through uniform porous medium, *Applied Mathematics and Mechanics*, Vol. 35, pp. 469-480, 2014.
- [36] H. Basha, G. J. Reddy, M. G. Reddy, Chemically reactive species of time-dependent natural convection couple stress fluid flow past an isothermal vertical flat plate, *Canadian Journal of Physics*, Vol. 97, No. 2, pp. 166-175, 2019.
- [37] M. G. Reddy, K. V. Reddy, O. Makinde, Hydromagnetic peristaltic motion of a reacting and radiating couple stress fluid in an inclined asymmetric channel filled with a porous medium, *Alexandria Engineering Journal*, Vol. 55, No. 2, pp. 1841-1853, 2016.
- [38] M. Awais, S. Saleem, T. Hayat, S. Irum, Hydromagnetic couple-stress nanofluid flow over a moving convective wall: OHAM analysis, *Acta Astronautica*, Vol. 129, pp. 271-276, 2016.
- [39] M. Farooq, S. Islam, M. Rahim, T. Haroon, Heat transfer flow of steady couple stress fluids between two parallel plates with variable viscosity, *Heat Transfer Research*, Vol. 42, No. 8, 2011.
- [40] M. Massoudi, I. Christie, Effects of variable viscosity and viscous dissipation on the flow of a third grade fluid in a pipe, *International Journal of Non-Linear Mechanics*, Vol. 30, No. 5, pp. 687-699, 1995.
- [41] O. Reynolds, IV. On the theory of lubrication and its application to Mr. Beauchamp tower's experiments, including an experimental determination of the viscosity of olive oil, *Philosophical transactions of the Royal Society of London*, No. 177, pp. 157-234, 1886.
- [42] A. Szeri, K. Rajagopal, Flow of a non-Newtonian fluid between heated parallel plates, *International Journal of Non-Linear Mechanics*, Vol. 20, No. 2, pp. 91-101, 1985.
- [43] M. Farooq, A. Khan, R. Nawaz, S. Islam, M. Ayaz, Y.-M. Chu, Comparative study of generalized couette flow of couple stress fluid using optimal homotopy asymptotic method and new iterative method, *Scientific Reports*, Vol. 11, No. 1, pp. 3478, 2021.
- [44] T. Chinyoka, O. D. Makinde, Analysis of transient generalized Couette flow of a reactive variable viscosity third-grade liquid with asymmetric convective cooling, *Mathematical and Computer Modelling*, Vol. 54, No. 1-2, pp. 160-174, 2011.